RICE UNIVERSITY

Elucidating the Roles of PEX19 and Prenylation in *Arabidopsis* Peroxisomes

by

Jerrad Michael Stoddard

A THESIS SUBMITTED IN
PARTIAL FULFILLMENT OF THE
REQUIREMENTS FOR THE DEGREE

Master of Arts

APPROVED, THESIS COMMITTEE:

Bonnie Bartel, Professor
Biochemistry and Cell Biology

Janet Braam, Professor, Chair
Biochemistry and Cell Biology

Mary Cindy Farach-Carson, Professor
Biochemistry and Cell Biology

Yousif Shamoo, Associate Professor
Biochemistry and Cell Biology

Jennifer Rudgers, Associate Professor
Ecology and Evolutionary Biology

Houston, Texas

May 2012

ABSTRACT

Elucidating the Roles of PEX19 and Prenylation in *Arabidopsis* Peroxisomes

by

Jerrad Michael Stoddard

Peroxisomes are organelles originating from the endoplasmic reticulum. Peroxisome biogenesis requires multiple peroxins, including PEX19, a prenylated protein that helps deliver peroxisomal membrane proteins in yeast and mammals. *Arabidopsis thaliana* PEX19 is encoded by two isogenes, *PEX19A* and *PEX19B*.

I demonstrate that *pex19A* and *pex19B* insertional mutants lack obvious abberant physiological phenotypes. I provide evidence that *pex19A pex19B* double mutants are inviable, that PEX19B is more abundant than PEX19A in young seedlings, that *Arabidopsis* PEX19 is farnesylated *in vivo*, and that YFP-PEX19 predominantly associates with what appears to be a subcellular membrane regardless of its prenylation state. I show that farnesyltransferase mutants apparently contain only non-prenylated PEX19 and lack phenotypes that would indicate inefficient peroxisome activity.

My analysis of PEX19 suggests that PEX19 prenylation is dispensable for peroxisome biogenesis, and has generated tools for future studies of the earliest steps in peroxisome biogenesis in plants.

ACKNOWLEDGEMENTS

Many people contributed to my success as a graduate student. I would like to thank:

My advisor Dr. Bonnie Bartel: Thank you for being a wonderful mentor and teacher. Without your dedication as a mentor, vast knowledge, and sage advice, I would not have been molded into the academic I am today. Thank you Bonnie for your encouragement, patience, and the exorbitant amount of feedback on my written documents. I am now a much better writer!

My present and former coworkers: Thank you to Lucia Strader and Naxhiely Martínez-Ramón for sharing your knowledge with me in the early days of my graduate career. Thank you to Wendell Fleming, Sarah Burkhart, Sarah Ratzel, Mauro Rinaldi and Lisa Farmer for being great colleagues and friends. I would also like to thank Adrianne Stone for her assistance in isolating transgenic and double mutant lines and Lynn Pauls for being the best undergraduate researcher that a graduate student could ask for!

My friends and family: Thank you for all your love and support. To my BCB friends, thank you for your open ears and never-ending feedback. Thank you to my partner, Bobby Cast, for always being by my side even though we have been apart for the last three years.

Lastly, I would like to thank the BCB faculty, especially my committee members, for providing excellent guidance and sharing their wisdom during my time here at Rice.

TABLE OF CONTENTS

FIGURES

TABLES

ABBREVIATIONS

2,4-D	2,4-dichlorophenoxyacetic acid
2,4-DB	2,4-dichlorophenoxybutyric acid
ABA	abscisic acid
CaaX	Cys-aliphatic-aliphatic-X
Col-0	Columbia
DTT	dithiothreitol
ER	endoplasmic reticulum
ERA1	enhanced response to abscisic acid 1
F1, F2, etc.	filial generation 1, 2, etc.
GGB	geranylgeranyltransferase I β-subunit
HPR	hydroxypyruvate reductase
HSC70	heat shock cognate protein
IAA	indole-3-acetic acid
IBA	indole-3-butyric acid
L*er*	Landsberg *erecta*
PCR	polymerase chain reaction
PEX	peroxin
PLP	pluripetala
PN	plant nutrient medium
PNS	plant nutrient medium supplemented with 0.5% sucrose
PFT	protein farnesyltransferase complex
PGGT	protein geranylgeranyltransferase complex

PMDH	peroxisomal malate dehydrogenase
PMP	peroxisomal membrane protein
PTS1/2	peroxisomal targeting signal type 1 and 2
T-DNA	transfer DNA
T1, T2, etc.	transformant generation 1, 2, etc.
Tris	Tris hydroxymethylaminoethane
Triton	octylpheoxypolyethoxyethanol polyethylene glycol-*p*-isooctylphenyl ether
YFP	yellow fluorescent protein

Chapter 1: Introduction

1.1. Peroxisomes

Peroxisomes are organelles that compartmentalize certain metabolic reactions. Unlike chloroplasts and mitochondria, peroxisomes do not contain their own DNA and are bound by a single lipid bilayer, suggesting that peroxisomes do not have an endosymbiotic origin. Two conserved functions of peroxisomes are fatty acid β-oxidation and hydrogen peroxide decomposition. In addition, peroxisomes sequester other metabolic processes and house the biosynthesis of numerous compounds, which vary depending on the organism.

1.1.A. The role of peroxisomes in *Arabidopsis*

In oilseed plants, such as *Arabidopsis thaliana*, peroxisomes are essential during seedling germination and establishment because stored fatty acids are β-oxidized and converted to sugar via the glyoxylate cycle, which is housed in specialized peroxisomes called glyoxysomes (reviewed by Graham, 2008). Additionally, peroxisomes house metabolism of indole-3-butyric acid (IBA) into its active form, indole-3-acetic acid (IAA) (Zolman *et al*., 2000; Strader *et al*., 2010). These processes are essential for seedling establishment and development, photorespiration, embryogenesis, and gametogenesis (reviewed by Hayashi and Nishimura, 2003).

1.1.B. Peroxisomal matrix protein import

Unlike chloroplasts and mitochondria, peroxisomes lack their own DNA. Thus, all peroxisomal proteins are nuclear-encoded and imported from the cytosol via a family of peroxin (PEX) proteins. After decades of research on peroxisome biogenesis in yeast,

mammals, and *Arabidopsis*, we have a working model that ascribes various roles to many of the identified PEX proteins involved in matrix protein import (Figure 1.1).

Peroxisomal matrix protein import begins with the cytosolic receptors, PEX5 and PEX7, which recognize proteins bearing a conserved C-terminal peroxisome targeting signal 1 (PTS1) or N-terminal PTS2 sequence, respectively. Upon cargo binding, PEX5 and PEX7 bind to the peroxisome membrane-docking complex, which includes PEX13 and PEX14 (reviewed in Brown and Baker, 2008). Once bound at the membrane, it is suggested that a dynamic pore consisting of PEX5 oligomers is created to allow translocation of the cargo into the peroxisome (Meinecke *et al*., 2010). In the peroxisome matrix, PTS2 proteins have their N-terminal recognition sequence proteolytically removed by DEG15, a PTS1 protein (Helm *et al.*, 2007; Schuhmann *et al.*, 2008). PEX5 is monoubiquitinated by the RING finger peroxin complex consisting of PEX2/10/12 and recycled into the cytoplasm for further rounds of import via the AAA-ATPase complex, PEX1 and PEX6 (reviewed in Lanyon-Hogg *et al*., 2010).

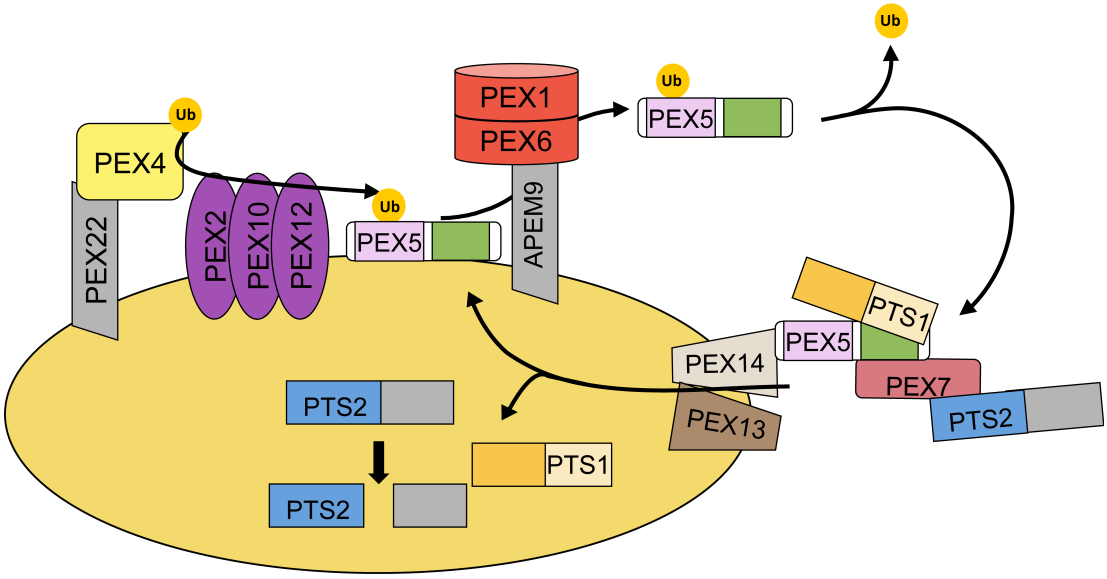

Figure 1.1. Model for peroxisomal matrix protein import in plants based on studies in plants, yeast, and mammals.

PTS1- and PTS2-tagged proteins are recognized by the cytosolic receptors PEX5 and PEX7, respectively. These cargo proteins and their receptors dock at the peroxisomal membrane via PEX13 and PEX14, and the cargo is translocated into the peroxisome. PEX4 is an E2 ubiquitin-conjugating enzyme, and PEX2/10/12 form a RING finger complex that is required for the monoubuitination of PEX5, which is then removed from the peroxisome into the cytosol by the AAA-ATPase PEX1 and PEX6 for further rounds of import. PEX7 recycling is not understood. Inside the peroxisome, the N-terminal PTS2 signal is removed, whereas the C-terminal PTS1 signal remains uncleaved.

1.1.C The role of PEX19 in peroxisome biogenesis

Although peroxisomal matrix protein import is relatively well characterized, the mechanisms of peroxisome biogenesis and peroxisomal membrane protein (PMP) import and assembly have not been fully explored. Peroxisomes can be formed either by division of existing peroxisomes or *de novo* by budding from the ER (reviewed by Fagarasanu *et al*., 2007). In *Saccharomyces cerevisiae,* PEX3[1] localizes to the ER to form foci that bud in a PEX19-dependent manner to produce pre-peroxisomes (Hoepfner *et al*., 2005). Inhibition of PEX19 specifically reduces PMP import in human fibroblasts (Jones *et al*., 2004), and nuclear localization of PEX19 also results in the localization of several PMPs to the nucleus (Sacksteder *et al*., 2000). Furthermore, yeast *pex3* or *pex19* mutants do not make peroxisomes (reviewed by Schliebs and Kunau, 2004), and *pex3* and *pex19* RNAi knockdown lines in *Arabidopsis* have enlarged peroxisomes and reduced matrix protein import activity (Nito *et al*., 2007), demonstrating important roles for PEX19 and PEX3 in peroxisome biogenesis.

Collectively, these data have led to a peroxisome biogenesis model that suggests that PEX19 functions as a molecular chaperone and/or import receptor for PMPs, such as PEX13 and PEX14 (Figure 1.2). Human PEX19 is predominantly cytosolic and binds and stabilizes multiple newly synthesized PMPs (Sacksteder *et al*., 2000; Jones *et al*., 2004) and shuttles them to the peroxisome membrane where PEX3 acts as a docking factor for PEX19 (Fang *et al*., 2004; Matsuzono *et al*., 2006). Although many reports suggest PEX19 targets PMPs to existing peroxisomes (Götte *et al*., 1998; Sacksteder *et al*., 2000; Fang *et al*., 2004; Matsuzono and Fujiki, 2006), there is evidence that PMPs are inserted

[1] Yeast proteins are conventionally indicated by the protein name followed by the letter "p" (e.g., Pex19p). To avoid confusion, I will use *Arabidopsis* and human nomenclature for proteins (e.g., PEX19) throughout this document.

into the ER membrane, and then transported to the peroxisome in *S. cerevisiae* (van der Zand *et al*., 2010). It also has been proposed that PEX19 could bind PMPs after ER membrane insertion to facilitate PMP congregation and/or peroxisome budding from the ER (reviewed in Ma *et al*., 2011). Thus, the role of PEX19 as a molecular chaperone and receptor for PMP import remains incompletely understood.

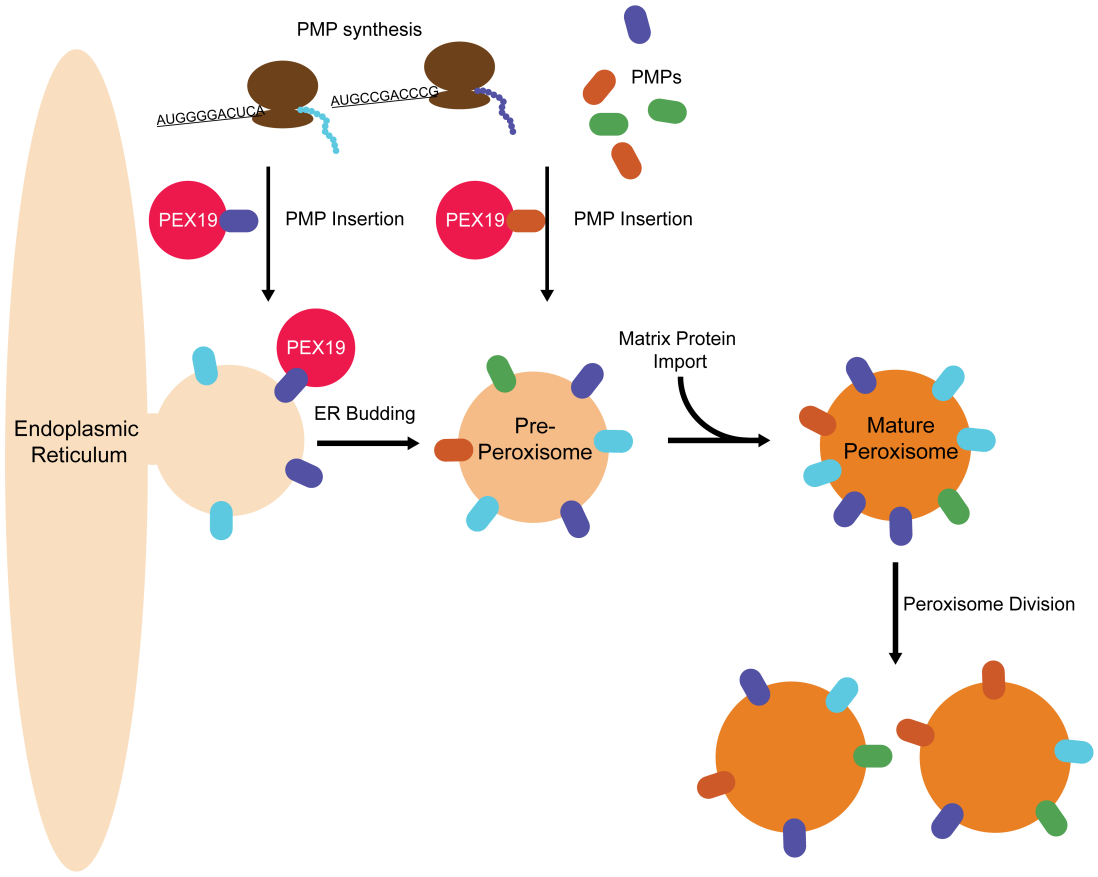

Figure 1.2. Model for PEX19 and peroxisome membrane protein interactions.

Peroxisomes are formed by vesicle budding from the ER and division of mature peroxisomes. PMPs are inserted into the ER membrane. PEX19 binds PMPs in the ER membrane to facilitate assembly of complexes and/or peroxisomal budding from the ER. Furthermore, PEX19 is able to insert newly synthesized PMPs into pre-peroxisomal vesicles.

1.1.D. Protein prenylation in *Arabidopsis*

I became interested in the role of protein prenylation in *Arabidopsis* peroxisome function when Lucia Strader, a former postdoc in the Bartel lab, found that the pleiotropic mutant *enhanced response to ABA* (*era1*; Cutler *et al*., 1996) was hypersensitive to the effects of IBA and the synthetic IBA analog 2,4-dichlorophenoxybutyric acid (2,4-DB), but not IAA and the synthetic IAA analog 2,4-dichlorophenoxyacetic acid (2,4-D), in root elongation assays. This result suggested that ERA1 is not acting generally in auxin signaling but specifically IBA-to-IAA and 2,4-DB-to-2,4-D conversion. Because *era1* is defective in the β-subunit of the protein farnesyltransferase (PFT) complex, these data suggest that protein prenylation negatively regulates peroxisomal IBA-to-IAA conversion.

era1 mutants have an enhanced response to abscisic acid (ABA), with increased stomatal closure and seed dormancy (Cutler *et al*., 1996), and an increase in the number of floral organs, which suggests meristem defects (Running *et al*., 1998; Bonetta *et al*., 2000; Yalovsky *et al*., 2000). However, a role for ERA1 in peroxisome function has not been previously suggested.

Protein prenylation can assist in targeting proteins to membranes and facilitate protein-protein interactions (reviewed by Crowell, 2000). Prenylation is the process of attaching a 15-carbon farnesyl or 20-carbon geranylgeranyl moiety to a protein (Figure 1.3). The *Arabidopsis* prenylation enzymes share a common α-subunit, PLURIPETALA (PLP), but have different β-subunits (ERA1 for the farnesylation complex; GGB for the geranylgeranylation complex). Both PFT and protein geranylgeranyltransferase (PGGT) complexes recognize a C-terminal CaaX

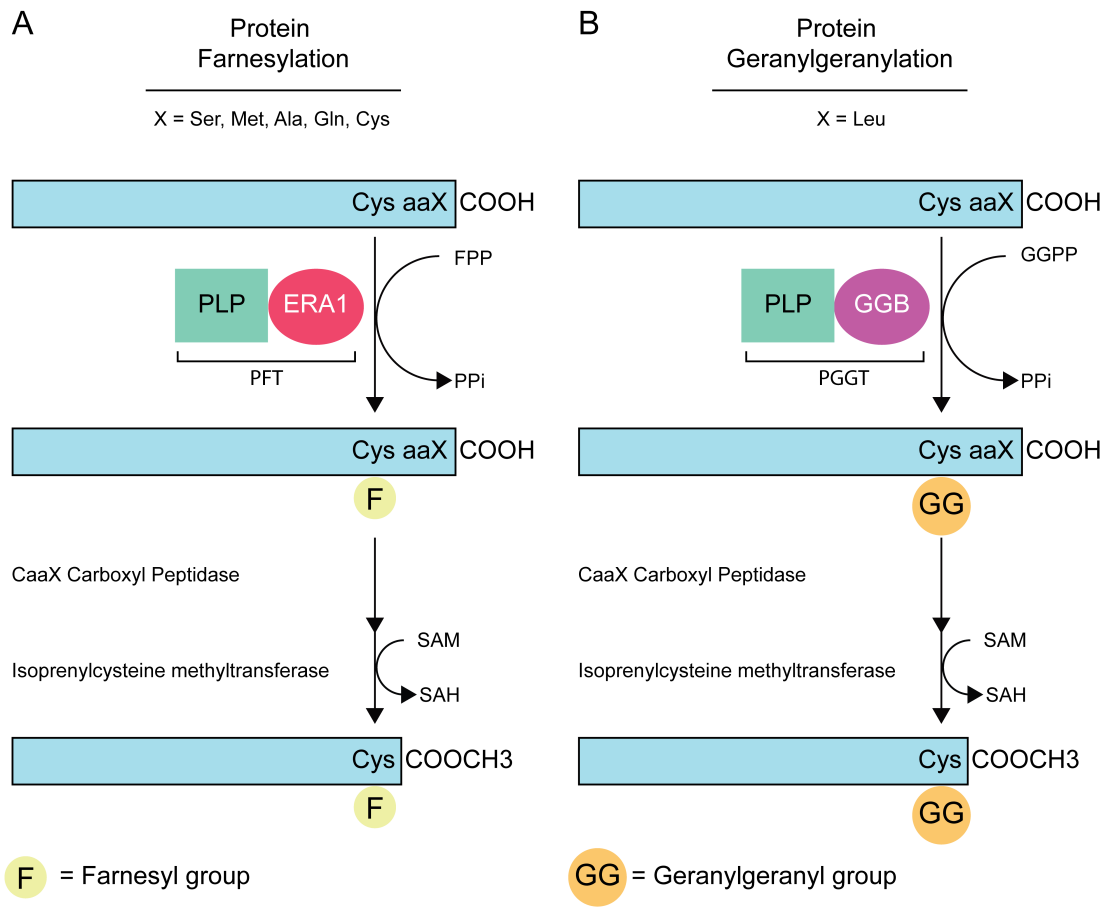

Figure 1.3. The process of protein prenylation.

A) Proteins terminating with a CaaX motif (Cys-aliphatic-aliphatic-X) are farnesylated by the protein farnesyltransferase (PFT) complex composed of PLP and ERA1.
B) CaaL proteins are geranylgeranylated by the protein geranylgeranyltransferase (PGGT) complex composed of PLP and GGB.

(Cys-aliphatic-aliphatic-X) tetrapeptide motif on target proteins, and the prenyl group is attached to cysteine via a thioether bond. The substrate specificities of PFT and PGGT complexes are determined by the terminal amino acid of the CaaX box. PFT usually prenylates proteins with an Ala, Cys, Gln, Met, or Ser as the terminal amino acid; PGGT almost exclusively prenylates proteins with Leu at the terminal position (Andrews *et al.*, 2010). However, these complexes are somewhat promiscuous. For example, the PFT complex can farnesylate proteins bearing a C-terminal CaaL motif, and the PGGT complex can geranylgeranylate proteins bearing a C-terminal CaaX motif (Andrews *et al.*, 2010).

era1 mutants, which are defective in farnesylation but not geranylgeranylation, have enlarged meristems and supernumerary floral organs (Running *et al*., 1998; Bonetta *et al*., 2000; Yalovsky *et al*., 2000). Interestingly, this phenotype is exaggerated in *plp* mutants (Running *et al*., 2004), which are defective in both prenylation processes, suggesting that targets that are normally farnesylated are instead geranylgeranylated or that the PGGT complex farnesylates targets in *era1* mutants, thereby partially rescuing farnesylation defects.

Database searches have identified 890 potential PFT and PGGT substrate proteins that contain a C-terminal CXXX motif, where X represents any amino acid, in *Arabidopsis*. Of these, PEX19 is the only predicted target known to function in peroxisomes, which led us to speculate that ERA1 was acting on peroxisome function by farnesylating PEX19.

1.1.E. PEX19 farnesylation

PEX19 is farnesylated in yeast (Götte *et al*., 1998; Rucktäschel *et al*., 2009) and mammals (James *et al*., 1994; Sacksteder *et al*., 2000; Mayerhofer *et al*., 2002); however, the functional significance of farnesylation on PEX19 function has generated an ongoing debate. For example, overexpression of nonfarnesylated PEX19 restores peroxisome activity and PMP localization to the peroxisome in *pex19* mutant Chinese hamster ovary cells (Vastiau *et al*., 2006), suggesting that farnesylation is not essential to PEX19 function. However, mutants defective in PEX19 farnesylation display significantly reduced steady-state concentrations of PMPs and decreased import of peroxisome matrix proteins in *S. cerevisiae* (Rucktäschel *et al*., 2009), suggesting that farnesylation enhances PEX19-PMP interactions.

1.1.F. *Arabidopsis* PEX19

Two *PEX19* homologs have been identified in *Arabidopsis*, *PEX19A* (At3g03490) and *PEX19B* (At5g17550). Although prenylation of PEX19 has not been demonstrated in *Arabidopsis*, the protein product of each isogene contains a C-terminal CaaM motif (CCIM for PEX19A and CCVM for PEX19B), suggesting that *Arabidopsis* PEX19 proteins will be farnesylated *in vivo*.

Nonfarnesylated *Arabidopsis* PEX19A can bind PEX10 *in vitro* (Hadden *et al*., 2006) and is thought to dimerize with other proteins, but it is not known if farnesylation modifies PEX19-PMP interactions. Thus, the functional significance of PEX19 farnesylation in *Arabidopsis* remains to be elucidated.

1.2. Tools for assaying peroxisome function in *Arabidopsis*

In *Arabidopsis*, mutations blocking peroxisome function often confer easily assayable phenotypes that reflect two β-oxidation pathways that occur in the peroxisome: fatty acid β-oxidation and indole-3-butyric acid (IBA) to indole-3-acetic acid (IAA) conversion.

1.2.A. Fatty acid β-oxidation

Arabidopsis seedlings use seed storage oils as an energy source during germination prior to developing photosynthetic abilities (reviewed in Graham, 2008) and require the catabolism of stored long-chain fatty acids during post-germinative growth to develop normally (Hayashi *et al*., 1998). Because many peroxisomal mutants do not efficiently β-oxidize fatty acids, these mutants typically require a supplemental energy source such as sucrose for normal development and are termed sucrose dependent (Hayashi *et al*., 1998; Zolman *et al*., 2000). Sucrose dependence can be monitored by measuring hypocotyl elongation in the dark (Zolman *et al*., 2000) or root elongation in the light (Zolman and Bartel, 2004).

1.2.B. IBA and IAA

IBA and IAA are naturally occurring auxins; the synthetic auxins, 2,4-dichlorophenoxybutyric acid (2,4-DB) and 2,4-dichlorophenoxy acetic acid (2,4-D) are functional analogues of IBA and IAA, respectively. Free IAA is released upon β-oxidation of IBA in the peroxisome, and IAA inhibits root elongation and promotes lateral root initiation (reviewed by Woodward and Bartel, 2005). The metabolism of 2,4-DB to 2,4-D similarly inhibits primary root elongation and promotes lateral root formation (Hayashi *et al*., 1998). Defects in PEX proteins can impair peroxisome

function, and many *Arabidopsis pex* mutants, such as *pex5-1*, are resistant to the inhibitory effects of IBA on root elongation and the stimulatory effects of IBA on lateral root proliferation (Zolman *et al*., 2000).

1.3. Overview

In this thesis, I will provide evidence that *pex19* single mutants do not have marked aberrant physiological phenotypes, PEX19B is more abundant than PEX19A in young seedlings, and that PEX19 is largely farnesylated *in vivo*. I also provide evidence that *PEX19* is an essential gene, because the *pex19A pex19B* double mutant does not appear to be viable. I show that the *eral* farnesyltransferase mutant appears to contain unmodified PEX19, suggesting that peroxisome biogenesis does not require PEX19 farnesylation. In addition, I determined that YFP-PEX19 predominantly associates with a subcellular membrane, perhaps the ER, regardless of its prenylation state.

Chapter 2: Materials and methods

2.1. Plant materials and growth conditions

For phenotypic assays, seeds were surface-sterilized by soaking seeds in a solution of 30% [v/v] bleach and 0.01% [v/v] Triton X-100 for 10 minutes, followed by two washes with sterile water and suspension in sterile 0.01% [w/v] agar (Last and Fink, 1988). Plants were grown on plant nutrient (PN) medium (Haughn and Somerville, 1986) supplemented with 0.5% [w/v] sucrose (PNS), hormones, or Basta (glufosinate-ammonium) as indicated. Seedlings were grown at 22°C under continuous white light, or yellow-filtered light (Stasinopoulos and Hangarter, 1990) for hormone-supplemented plates.

2.2. Phenotypic analysis

2.2.A. Root elongation

Seedlings were grown under constant white light for 8 days on PN or PNS supplemented with hormones as indicated. Roots were measured to the nearest millimeter and means and standard errors were calculated using Microsoft Excel.

2.2.B. Lateral root proliferation

Seedlings were grown on PNS for 4 days under white light at 22°C then transferred to new plates containing hormone or an equal volume of ethanol for the mock treatment for another 4 days under yellow-filtered light (Stasinopoulos and Hangarter, 1990). Roots were measured to the nearest millimeter and lateral roots were counted using a dissecting microscope. The quotient of lateral roots per millimeter was calculated for each seedling and the mean of this value and standard errors were calculated using Microsoft Excel.

2.2.C. Sucrose dependence in the dark

Seedlings were grown on PN or PNS for one day under white light. Plates were then wrapped in foil and incubated for an additional 4 days. Hypocotyls were measured to the nearest millimeter and means and standard errors were calculated using Microsoft Excel.

2.3. Genetic analysis of mutants

2.3.A. Plant DNA isolation

DNA was obtained from plant tissue as described (Celenza *et al.*, 1995). Briefly, a leaf was placed in a 1.5 mL microcentrifuge tube and frozen on dry ice. Frozen tissue was ground with a pestle followed by the addition of 10 μL of 0.5 N NaOH and placement in a 100°C sand bath for 30 seconds. The solution was then neutralized with 100 μL of 0.2 M Tris pH 8.0 with 1 mM EDTA pH 8.0.

2.3.B. *pex19* insertional mutant isolation

Insertions of Transfer-DNA (T-DNA) sequences in genes of interest were used in these studies to examine the effects of *PEX19* gene disruption. *pex19A-1* (SALK_020100C; Alonso *et al.*, 2003) and *pex19B-1* (SAIL_76_C06; Sessions *et al.*, 2002) T4 seeds were obtained from the *Arabidopsis* Biological Resource Center (Ohio State University). Upon arrival, seeds were surface-sterilized, plated, and transferred to soil. Gene specific primers (Table 2.1) were designed to span the T-DNA insertion to genotype *pex19A-1* (amplification with PEX19A-1 and PEX19A-2 yields a 619 bp product from *PEX19*; PEX19A-1 and LB1-SALK yields a 698 bp product from the transgene) and *pex19B-1* (amplificiation with PEX19B-1 and PEX19B-2 yields a 593 bp

Table 2.1. Sequences of oligonucleotides used to determine genotypes of *pex19* mutants.

Name	Sequence (5' to 3')
PEX19A-1	CCTAAGGAAAATGGCGAACAGTCACACC
PEX19A-2	AGGCAGCTGCTTAGAAGAAATGG
PEX19B-1	AAAAATGGGCTTACGACACAACAC
PEX19B-2	TCCCACCAAAAACATAACAGAACCTC
LB1-SALK	CAAACCAGCGTGGACCGCTTGCTGCAACTC
LB2-SAIL	GCTTCCTATTATATCTTCCCAAATTACCAATACA

product from *PEX19*; PEX19B-1 and LB2-SAIL yields a 635 bp product from the transgene).

2.3.C. Determining the size of the *era1-2* lesion

The *era1-2* allele was generated by fast-neutron mutagenesis (Cutler *et al.*, 1996) and was reported to result in a 7.5 kb deletion spanning the *ERA1* gene based on Southern blot analysis (Cutler *et al.*, 1996). To create a PCR-based assay to genotype *era1-2*, I first determined where the deletion began and ended. I designed numerous primer pairs upstream of *ERA1* translation initiation site (ATG) and downstream of the *ERA1* translation stop site (TGA) (Table 2.2). PCR amplifications were setup using the various primer pairs and wild-type or *era1-2* DNA as the template. If the PCR using both wild type and *era1-2* were successful, then I concluded that the amplified region was present in *era1-2*. However, if a PCR was successful when wild-type DNA was used but unsuccessful when *era1-2* DNA was used as a template, then I concluded that that region was absent in *era1-2*. After narrowing the region where the deletion began and ended, I PCR-amplified across the deletion in *era1-2* (upERA1-27 + downERA1-9) and sequenced the resulting product. By comparing this sequence to the wild-type reference sequence, I determined that the *era1-2* deletion is 26.5 kb and spans a total of 10 genes, including *ERA1*. I designed primers to genotype *era1-2* (upERA1 + downERA1) that amplify a 410 bp fragment from *era1-2* and fail to amplify a product from *ERA1*.

Table 2.2. Primer pairs used to determine the size of the *era1-2* lesion.

Primers	Expected product size	Position in relation to *ERA1* ATG	Wild-type product	*era1-2* product
upERA1-15 + upERA1-16	485 bp	-27.5 kb	+	+
upERA1-19 + upERA1-20	593 bp	-25.9 kb	+	+
upERA1-21 + upERA1-22	602 bp	-24 kb	+	+
upERA1-25 + upERA1-26	465 bp	-23.4 kb	+	-
upERA1-23 + upERA1-24	458 bp	-22.9 kb	+	-
upERA1-17 + upERA1-18	429 bp	-21.9 kb	+	-
upERA1-13 + upERA1-14	459 bp	-16.5 kb	+	-
upERA1-9 + upERA1-10	451 bp	-13.2 kb	+	-
upERA1-7 + upERA1-8	441 bp	-11.5 kb	+	-
upERA1-5 + upERA1-6	458 bp	-10.4 kb	+	-
upERA1-1 + upERA1-2	456 bp	-8.4 kb	+	-
upERA1-3 + upERA1-4	445 bp	-1.7 kb	+	-
ERA1-5 + ERA1-4	280 bp	+858 bases	+	-
ERA1-6 + ERA1-7	300 bp	+3 kb	+	-
downERA1-5 + downERA1-6	422 bp	+3.4 kb	+	-
downERA1-1 + downERA1-2	437 bp	+5.3 kb	+	+
upERA1-27 + down ERA1-9	1313 bp	N/A	-	+
upERA1 + downERA1	410 bp	N/A	-	+

2.3.D. *ggb* and *plp* insertional mutant isolation

ggb-2 (SALK_040904; Alonso *et al.*, 2003), *ggb-3* (SALK_015072; Alonso *et al.*, 2003) and *plp-3* (SALK_015079; Alonso *et al.*, 2003) T4 seeds were obtained from the *Arabidopsis* Biological Resource Center (Ohio State University). Upon arrival, seeds were surface-sterilized, plated, and transferred to soil. Gene specific primers (Table 2.3) were designed to span the T-DNA insertion to genotype *ggb-2* (PCR with GGB-1 and GGB-2 yields a 570 bp product from *GGB*; GGB-2 and LB1-SALK yields a ~240 bp product from the transgene) and *ggb-3* (amplification with GGB-1 and GGB-2 yields a 570 bp product from *GGB*; GGB-2 and LB1-SALK yield a ~610 bp product from the trangene) and *plp-3* (amplification with PLP-1 and PLP-2 yields a 595 bp product from *PLP*; PLP-1 and LB1-SALK yields a ~600 bp product from the transgene). I determined that the *ggb-2* insertion site is in the first exon, the *ggb-3* insertion site is 184 bp upstream of the start site, and the *plp-3* insertion site is 174 bp upstream of the start site.

2.4. Recombinant DNA methods

2.4.A. Generating constructs using the Gateway system

Cloning was conducted using the Gateway recombination system (Invitrogen), which bypasses the need for restriction enzymes and ligation. Gateway entry clones carrying *PEX19A* (G66139) and *PEX19B* (G13403) cDNAs in the pENTR223 vector were obtained from the ABRC (Ohio State University) and sequenced.

To create PEX19ΔCaaX and PEX19-CaaL constructs, the cDNAs were PCR-amplified using PEX19(A/B)-CACC and PEX19(A/B)-noCaaX or PEX19A/B-CaaL (Table 2.4), purified using a DNA Clean & Concentrator Kit (Zymo Research), and inserted into the pENTR/D-TOPO directional cloning vector (Invitrogen). The protocol

Table 2.3. Sequences of primers used to determine genotypes of prenylation mutants.

Name	Sequence (5' to 3')
GGB-1	ATAAAATAAAATCAATGCCCCCAATG
GGB-2	GCGCCGAGAAAATGAAGACCCGAG
PLP-1	ACTCTTAAAATTATCCTTGTTG
PLP-2	CGAAATTCATGTTCCCCGACTC
LB1-SALK	CAAACCAGCGTGGACCGCTTGCTGCAACTC
upERA1	AAAAGTCTGCATAACCGTAACC
downERA1	GGAAACCTTGAAAATAACAC

Table 2.4. Sequences of oligonucleotides used to create PEX19 constructs

	Name	Sequence (5' to 3')
Forward primers	PEX19A-CACC	CACCATGGCGAACAGTCACACCGATGAC
	PEX19B-CACC	CACCATGGCCAACGATACTCACACCG
Reverse primers	PEX19A-noCaaX	GATACATCAATTTGGCGAGGAC
	PEX19B-noCaaX	ATCAATTTGGTGAAGACTC
	PEX19A-CaaL	TCACAGGATACAGCAATTTGGCGAGGAC
	PEX19B-CaaL	TCACAGTACACAACAATTTGGTGAAGACTC

* Note: There are no reverse primers for wild type PEX19 cDNA because the cDNA clones obtained from the ABRC were already in the pENTR vector.

was followed as stated in the Invitrogen manual except the reaction was incubated overnight instead of five minutes.

The cDNA was subcloned from the pENTR vector into various plant destination vectors (Earley *et al.*, 2006) using Gateway recombination to create constructs for *Agrobacterium*-mediated plant transformation (Table 2.5). The pENTR-target vector was digested with MluI to prevent selection of the entry vector because both entry and destination vectors confer kanamycin resistance. After enzymatic digestion, the DNA was purified using a DNA Clean & Concentrator Kit (Zymo Research) and incubated with the destination vector in TE Buffer and LR Clonase II (Invitrogen) overnight. Then, 1 μL of Proteinase K solution (Invitrogen) was added and incubated for 10 minutes at 37°C. The destination vector was transformed into NEB5α (New England Biolabs), sequenced to verify the insert, and transformed into *Agrobacterium tumefaciens* strain GV3101 (Koncz *et al.*, 1992).

2.4.B. *Escherichia coli* transformation and growth conditions

NEB5α (New Englad Biolabs) chemically competent cells were used in this study. Cells were thawed on ice and 2 μL of DNA was added to cells and incubated on ice for 10 minutes. Transformation mixtures were heat shocked at 42°C for 30 seconds followed by the addition of 250 μL of SOC. Cells were allowed to recover for 1 hour while gently shaking at 37°C. Transformed cells were selected on kanamycin (50 μg/mL) and grown overnight at 37°C.

2.4.C. *Agrobacterium tumefaciens* transformation and growth conditions

Constructs (Table 2.5) were transformed in *Agrobacterium tumefaciens* strain GV3101 (Koncz *et al.*, 1992) using electroporation (Ausubel *et al.*, 1995). Transformants

Table 2.5. Bartel lab strain numbers for plasmids used in this study.

Insert	Destination Vector			
	pEG100 (no tag)	pEG104 (N-terminal YFP tag)	pEG201 (N-terminal HA tag)	pEG203 (N-terminal myc tag)
PEX19A	2959* *2498*	2956 *2958*	2961* *2502*	
PEX19AΔCaaX	2750 *2895*	2752 *2896*		2754 *2897*
PEX19B	2960* *2499*	2957 *2963*	2962* *2503*	
PEX19BΔCaaX	2751 *2898*	2753 *2946*	2755 *2899*	

Each construct was transformed into NEB5α (strain number listed on top) and GV3101 (strain number italicized and below the NEB5α strain number). An asterisk indicates constructs that were made by Lucia Strader, a former post doc in the Bartel lab.

were selected for kanamycin (50 μg/mL) and gentamycin (50 μg/mL) resistance after growing several days at room temperature. Bacterial strains were stored at -80°C in 50% [v/v] glycerol.

2.4.D. *Arabidopsis thaliana* transformation and growth conditions

Wild type Col-0 plants were grown at 22°C under continuous white light before being transformed with GV3101 strains carrying the constructs of interest via the floral dip method (Clough and Bent, 1998).

After harvesting T_1 seeds, transformants were selected on PN medium supplemented with 7.5 μg/mL BASTA. BASTA-resistant transformants were transferred to soil. T_2 seeds were plated on PN medium supplemented with 7.5 μg/mL BASTA, and about 12 BASTA resistant individuals were moved to soil. For most constructs, T_3 lines were checked for BASTA resistance to identify homozygous lines, and these lines were used in Western and phenotypic analyses. However, YFP-PEX19 localization and immunoblotting studies were conducted on segregating T_2 lines.

2.5. PEX19 antibody development

Lyophilized *PEX19B* cDNA in the pENTR223 (Gateway clone G13403) was submitted to Proteintech Group (Chicago, IL) for protein synthesis, purification, and polyclonal antibody production and affinity purification. Briefly, the cDNA was subcloned into a T-HIS expression vector, expressed in bacterial strain BL21 (DE3), and the synthesized protein was purified and injected into two rabbits. Antibody production was verified from a test bleed, and the final production bleed from rabbit #1 was affinity purified.

2.6. Western blot analysis

Protein was extracted by grinding tissue from 8-day-old seedlings that were grown under continuous white light at 22°C on PNS. An equal volume of NuPAGE 2x loading buffer (Invitrogen, Carlsbad, CA) was mixed with the ground tissue and centrifuged at 13,200 rpm for 5 minutes at 4°C. Following centrifugation, 10 μL of the supernatant was transferred to a new tube with 1 μL of 0.5 M DTT and the mixture was boiled for 5 minutes in a 100°C sand bath. The samples were then loaded onto NuPAGE 10% or 12% [w/v] Bis-Tris gels (Invitrogen) next to broad range prestained protein markers (P7708S, New England Biolabs, Beverly, MA) and Cruz Markers (Santa Cruz Biotechnology, Santa Cruz, CA). After electrophoresis using NuPAGE MOPS SDS running buffer (Invitrogen), proteins were transferred at 24 V to a Hybond ECL nitrocellulose membrane (Amersham Pharmacia Biotech, Piscataway, NJ) for 35 minutes in NuPAGE transfer buffer (Invitrogen). Membranes were blocked for 1 hour with 8% [w/v] non-fat dry milk in Tween Tris-Buffered Saline (Ausubel *et al.*, 1999) then incubated overnight at 4°C with rabbit anti-PEX5 (1:100 dilution; Zolman and Bartel, 2004), rabbit anti-PEX7 (1:2500 dilution; Ramón and Bartel, 2010), rabbit anti-PMDH2 (1:2000 dilution, Pracharoenwattana *et al.*, 2007), rabbit anti-PEX14 (1:10000 dilution, Lingard and Bartel, 2009), rabbit anti-PEX19B (1:2000 dilution, see section 2.5), rabbit anti-HPR (1:1000 dilution; Kleczkowski and Randall, 1988), rabbit anti-GFP (1:300 dilution; Clontech Laboratories, Mountain View, CA) or mouse anti-HSC70 (1:500 dilution, SPA-817, StressGen Biotechnologies, San Diego, CA) as primary antibodies. Horseradish peroxidase-linked goat anti-rabbit or anti-mouse immunoglobulin G (IgG) (SC-2030 or SC-2031, Santa Cruz Biotechnology) were used as secondary antibodies.

Horseradish peroxidase was visualized using LumiGLO (Cell Signaling Technology, Danvers, MA).

2.7 Microscopy

Plant lines expressing YFP-PEX19 (Table 2.5) were grown on sucrose-supplemented medium at 22°C for 6 days under white light. Prior to imaging, seedlings were submerged in 10 μg/mL propidium iodide for approximately 30 minutes to stain cell walls. Samples were mounted on a microscope slide with sterile MilliQ water. Confocal images were obtained using a Zeiss LSM 710 laser scanning microscope equipped with a 100X oil immersion lens. YFP and propidium iodide were excited using a 488 nm argon laser. Bandpass emission filters of 516-576 nm and 662-730 nm were used to detect YFP and propidium iodide, respectively.

Chapter 3: Characterization of *pex19* loss of function mutants

Arabidopsis PEX19 is encoded by two isogenes, *PEX19A* and *PEX19B*, which are 82% identical at the nucleotide level and encode proteins that are 79% identical at the amino acid level. The facts that PEX19 proteins are highly homologous and no *pex19* allele has ever been isolated from a forward genetics screen suggest that these proteins function redundantly. Because PEX19 is thought to function as the cytosolic receptor/chaperone for PMPs, we expected *pex19* mutants to display peroxisome-defective phenotypes. This chapter summarizes the phenotypic assays that I conducted to characterize *pex19* loss-of-function mutants.

3.1. *pex19* T-DNA insertional mutants do not have any abberant phenotypes

The positions of the T-DNA insertion alleles used in these studies are depicted in Figure 3.1. Because *pex* mutants commonly have physiological phenotypes that reflect defects of peroxisome function, such as sucrose dependence and IBA resistance, I initially characterized *pex19* insertion mutants using these assays. I used the previously characterized *pex4-1* (Zolman *et al*., 2005) and *pex5-1* (Zolman *et al*., 2000) mutants as controls representing mutants with moderate peroxisome defects.

3.1.A. IBA response assays

Peroxisome-defective mutants typically cannot convert IBA to IAA efficiently, resulting in long primary roots with few lateral roots following growth when grown on IBA. I observed that both *pex19* single mutants were sensitive to root elongation inhibition (Figure 3.2) and lateral root promotion (Figure 3.3) by IBA, suggesting that peroxisome function in these single mutants is not markedly impaired.

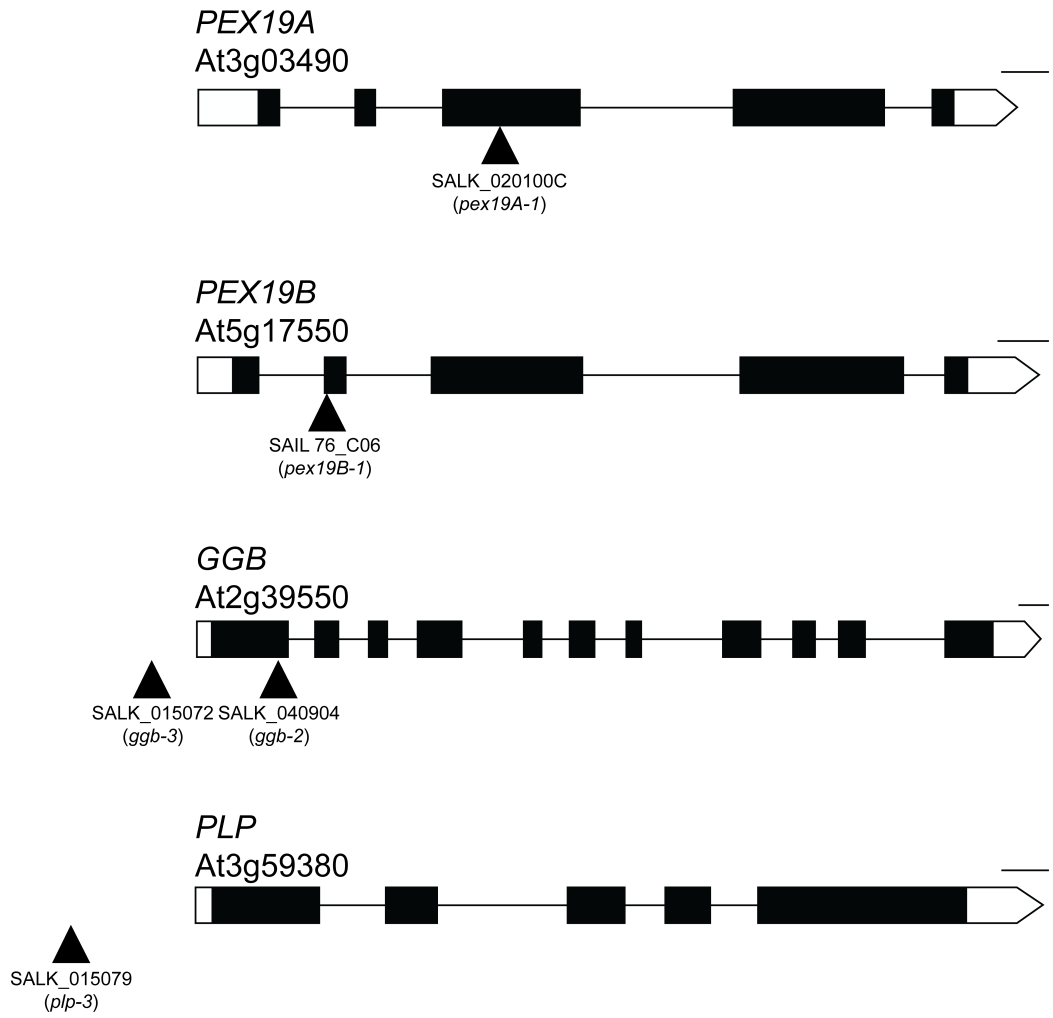

Figure 3.1. Schematic of *PEX19A, PEX19B, GGB,* and *PLP* genes.

T-DNA insertion sites are indicated by triangles, 5' and 3' untranslated regions are indicated in white, exons are indicated by black rectangles, and introns are indicated by lines. Insertion sites are denoted by triangles; *ggb-3* and *plp-3* insertion sites are 184 bp and 300 bp upstream of the ATG translation start site, respectively. Scale bar = 100 bp.

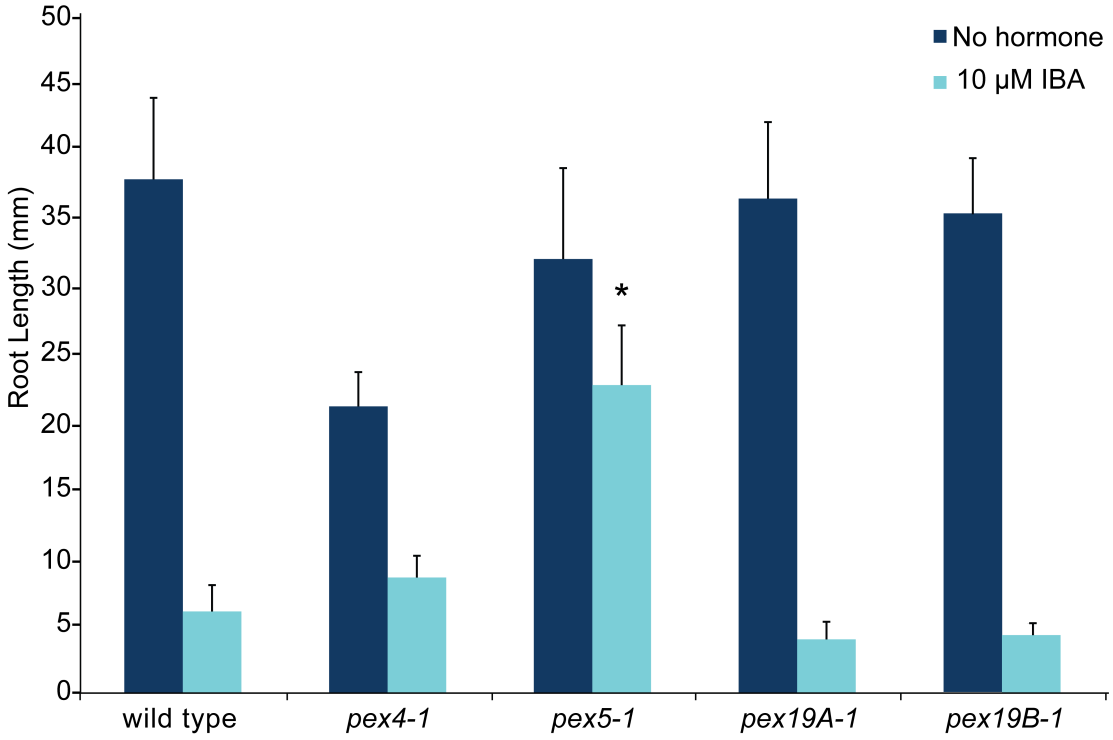

Figure 3.2. *pex19* single mutants are sensitive to inhibition of root elongation by IBA.

Seeds were grown on medium with or without IBA under yellow-filtered light for eight days. Plants were removed and root length was measured. Bars show mean + SD; n ≥ 8. *pex19A-1* and *pex19B-1* are derived from original stock center lines and have not been backcrossed. An asterisk denotes a value significantly different than the wild type (unpaired Student's *t* test, two-tailed p value ≤ 0.001).

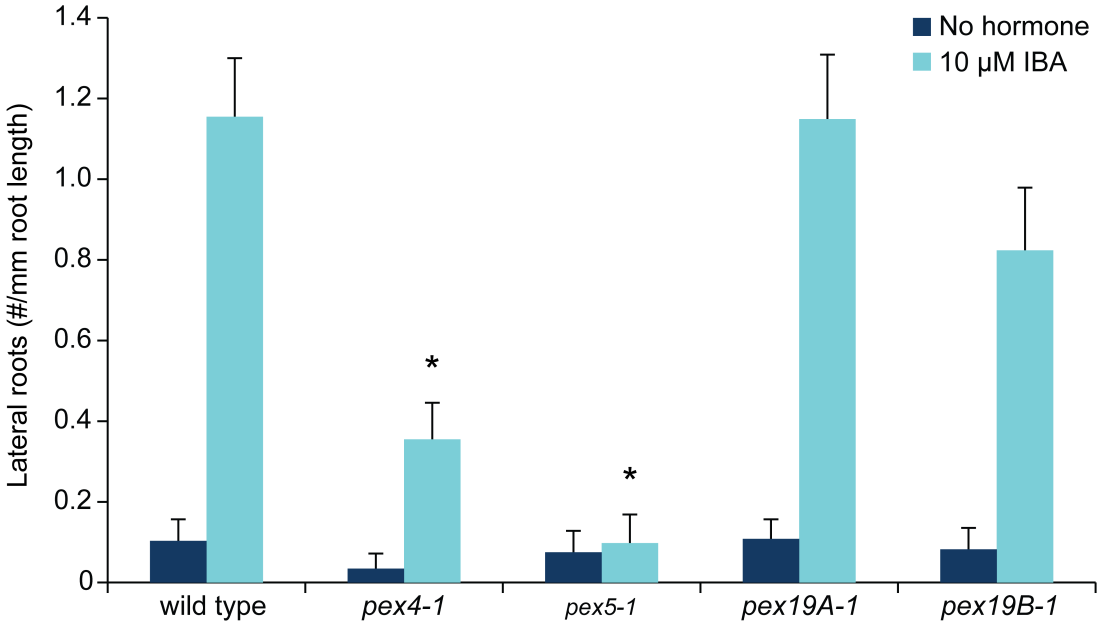

Figure 3.3. *pex19* single mutants are sensitive to lateral root promotion by IBA.

Four-day-old seedlings were transferred from medium without hormone to medium containing IBA or no hormone. Plants were removed after four additional days and root length was measured and lateral roots were counted. Bars show mean + SD; $n \geq 8$. *pex19A-1* and *pex19B-1* are derived from original stock center lines and have not been backcrossed. Asterisks denote values significantly different than the wild type (unpaired Student's *t* test, two-tailed p value ≤ 0.001).

3.1.B. Sucrose dependence assays

In addition to defects in IBA-to-IAA conversion, peroxisome-defective mutants often cannot efficiently catabolize stored fatty acids after germination, which results in delayed development that be rescued by the addition of sucrose (Hayashi *et al.*, 1998; Zolman *et al.*, 2000). However, *pex19A-1* and *pex19B-1* did not display sucrose dependence in the dark (Figure 3.4) but resembled wild type. Although the mean root length of *pex19A-1* seedlings was significantly different when grown in the presence versus the absence of sucrose in the dark (Figure 3.4), the error bars overlap and suggest that *pex19A-1* is not sucrose dependent in the dark.

3.1.C. Lethality of the *pex19A pex19B* double mutant

To isolate a *pex19A pex19B* double mutant, we crossed the *pex19* single mutants and genotyped 46 F2 individuals. However, I did not recover a double mutant, suggesting that the double mutant is inviable during embryogenesis, as has been reported for several other *Arabidopsis* peroxin mutants (Lin *et al*., 1999; Hu *et al*., 2002; Schuhmann *et al*., 2003; Sparkes *et al*., 2003; Fan *et al*., 2005).

Progeny of F2 individuals genotyped as *pex19A/pex19A;PEX19B/pex19B* or *PEX19A/pex19A;pex19B/pex19B* were plated on 10 μM IBA and incubated under yellow-filtered light at 22°C. After 8 days, each seedlings was measured and DNA was extracted and the *pex19A* and *pex19B* genotypes were determined using PCR. Again, after screening through 108 individuals, I did not recover any *pex19A pex19B* homozygous double mutants in this experiment. Surprisingly, I observed that *PEX19A/PEX19A;pex19B/pex19B* individuals were somewhat IBA resistant and that this

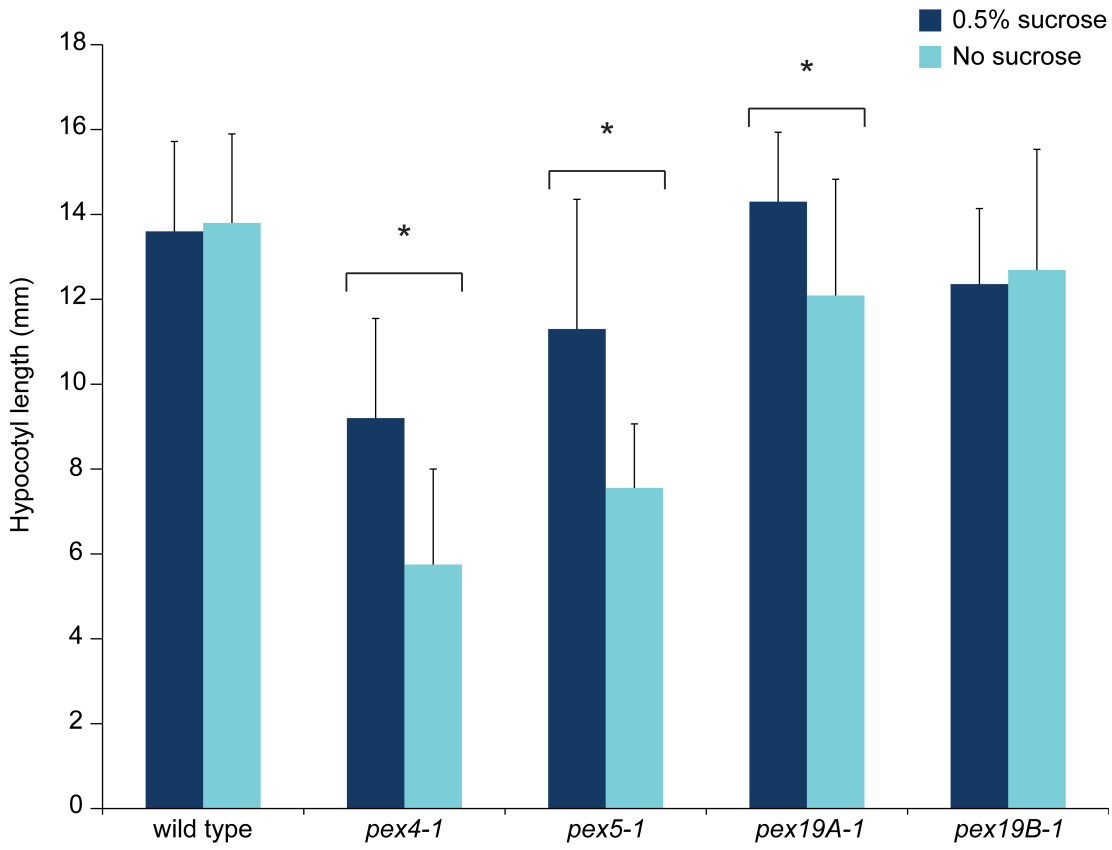

Figure 3.4. *pex19* single mutants are not sucrose dependent in the dark.

Seedlings were grown on medium with or without 0.5% [w/v] sucrose for 1 day in the light followed by 4 days in the dark. Bars show mean hypocotyl length + SD; n ≥ 8. *pex19A-1* and *pex19B-1* are derived from original stock center lines and have not been backcrossed. Asterisks denote values that are significantly different (unpaired Student's *t* test, two-tailed p value ≤ 0.01).

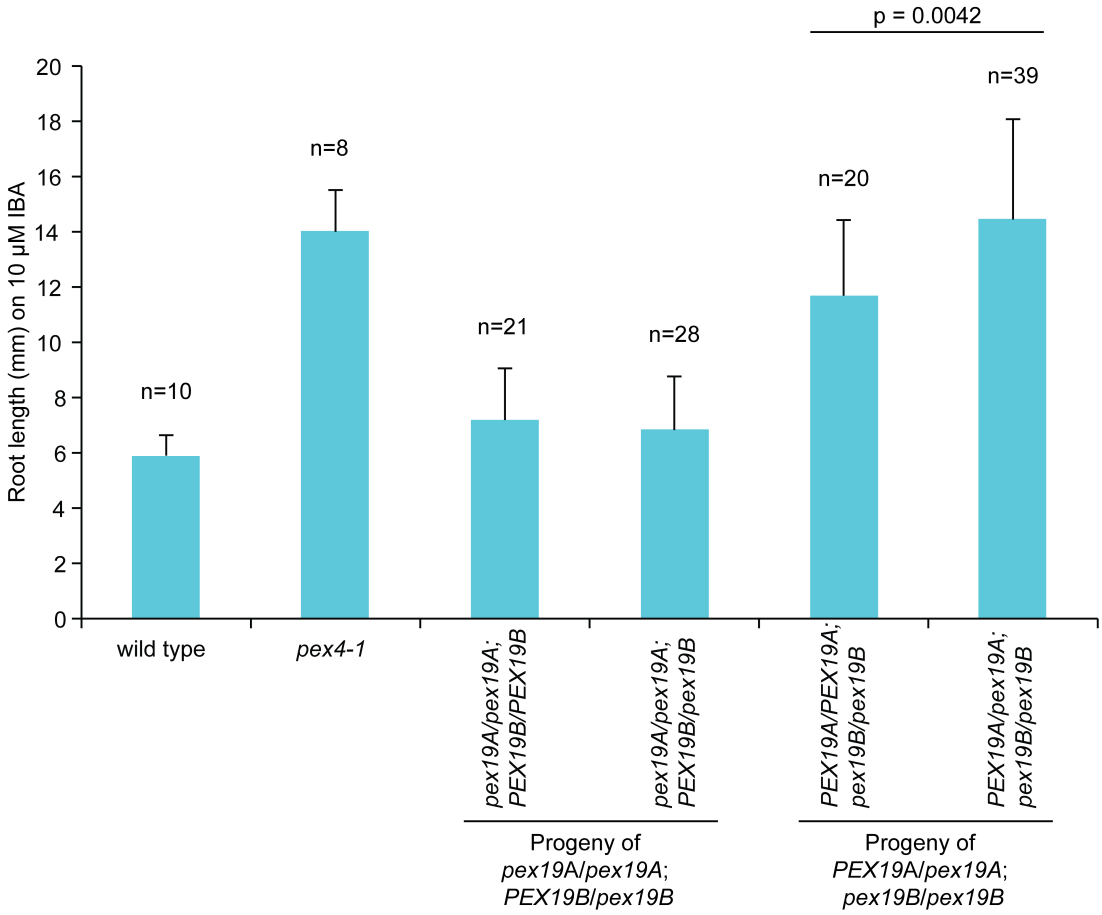

Figure 3.5. IBA response in plants homozygous for one *pex19* mutant and heterozygous for the other.

Seedlings were grown on medium supplemented with IBA (10 µM). After eight days, plants were removed and root lengths were measured. After measurement, DNA was prepared from individual seedlings and the *pex19A* and *pex19B* genotypes were determined using PCR. No *pex19A/pex19A*;*pex19B/pex19B* homozygous double mutants were recovered. Bars show mean + SD. An unpaired t-test was employed for statistical analysis after an F-test for equal variance confirmed that the *PEX19A/PEX19A;pex19B/pex19B* and *PEX19A/pex19A;pex19B/pex19B* samples have equal variances.

IBA resistance was enhanced by reduced PEX19A dosage (Figure 3.5). In contrast, the *pex19A/pex19A*; *PEX19B/PEX19B* and *pex19A/pex19A*; *PEX19B/pex19B* mutants resembled wild type in this assay (Figure 3.5) consistent with my analysis of the original *pex19A/pex19A* mutant (Figure 3.2). Future experiments with backcrossed *pex19B* mutants are needed to resolve the observed discrepancy in *pex19B* IBA response phenotypes (Figure 3.2 vs. Figure 3.5).

3.2. PEX protein accumulation in *pex19* mutants

Because PEX19 is thought to act as the cytosolic receptor for PMPs in yeast (reviewed by Fujiki *et al*., 2006) and mammals (Sacksteder *et al*., 2000; Jones *et al*., 2004), *pex19* mutants may have decreased PMP steady-state concentrations due to PMP aggregation and degradation, which would subsequently lead to matrix protein import defects. Using immunoblot analysis, I observed that 3-, 5-, and 8-day-old *pex19B-1* single mutants had very little PEX19 protein compared to wild type (Figure 3.6). Despite this reduced PEX19 accumulation, *pex19B* single mutants did not appear to have altered PEX5, PEX7, or PEX14 protein accumulation (Figure 3.6).

3.3. PTS2 processing analysis in *pex19* mutants

Because type 2 peroxisome targeting signals (PTS2) are proteolytically cleaved upon matrix protein import (Helm *et al*., 2007; Schuhmann, 2008), we can indirectly assess protein import by using immunoblotting to monitor the removal of the PTS2 signal from peroxisomal malate dehydrogenase (PMDH). I observed that *pex19A-1* and *pex19B-1* single mutants did not have discernable PTS2 processing defects (Figure 3.6), suggesting that peroxisomal matrix protein import was not impaired in these mutants.

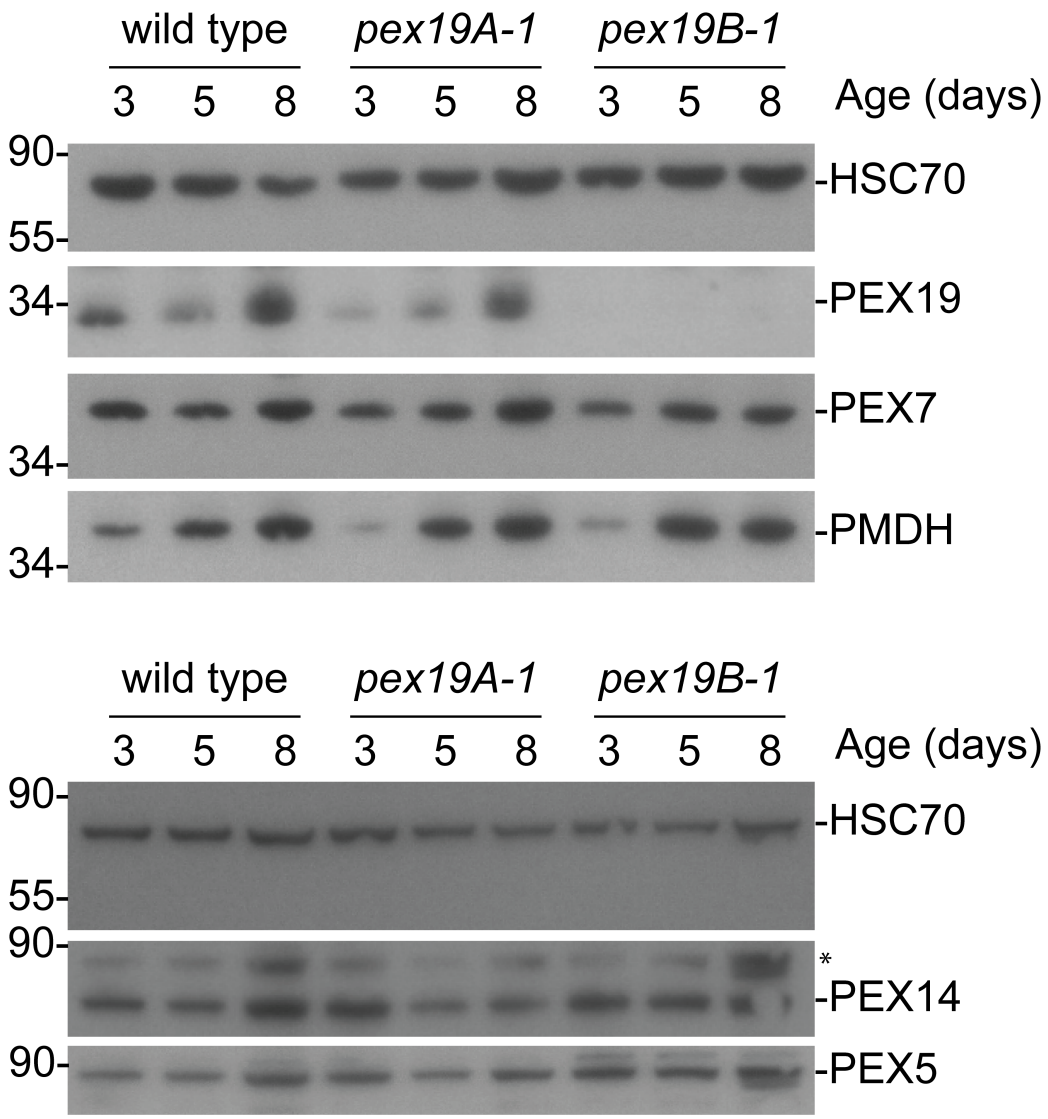

Figure 3.6. Temporal protein accumulation in *pex19* single mutants.

Seedlings were grown on sucrose-supplemented medium for 3, 5, or 8 days under white light at 22°C . Protein was extracted from 8-10 seedlings, loaded into duplicate gels, separated by 12% [w/v] SDS-PAGE and analyzed by immunoblotting with the indicated antibodies. *pex19A-1* and *pex19B-1* are derived from original stock center lines and have not been backcrossed. An asterisk indicates residual PEX5 signal. The positions of molecular weight markers are indicated on the left (in kDa).

3.4. Isolation and characterization of double mutants

We crossed a variety of peroxin mutants to *pex19* single mutants to assess genetic interactions between *pex19* and other *pex* mutants. Individuals from each line were genotyped by for *pex19* and the *pex* allele using PCR. Progeny from homozygous individuals were plated on 10 μM IBA, and IBA response was assessed after 8 days. It was observed that *pex19A* did not appear to alter IBA response when combined with *pex5-1* and *pex6-1* (Figure 3.7; Adrianne Stone, personal communication). However, *pex19B* appeared to noticeably enhance the IBA resistance of *pex7-1* (Figure 3.7; Adrianne Stone, personal communication). This clear enhancement of *pex7-1* by *pex19B-1* suggests that the reduced PEX19 level observed in *pex19B-1* (Figure 3.6) is sufficient to reduce peroxisome function in a sensitized background. Because some of the *pex* mutants (e.g., *pex14-2* and *pex16-1*) were fully resistant to the level of IBA used in this assay, this experiment will need to be repeated using a higher IBA concentration.

3.5. Characterizing prenylation mutants

Farnesyltransferase (PLP and ERA1) and geranylgeranyltransferase (PLP and GGB) complexes are known to be promiscuous. For example, the PFT complex is capable of farnesylating proteins bearing a C-terminal CaaL motif, and the PGGT complex is capable of geranylgeranylating proteins bearing a C-terminal CaaX motif (Andrews *et al.*, 2010). Furthermore, *era1* mutants, which are defective in farnesylation but not geranylgeranylation, have enlarged meristems and supernumerary floral organs (Bonetta *et al*., 2000; Yalovsky *et al*., 2000). Interestingly, this phenotype is exaggerated in *plp* mutants (Running *et al.*, 2004), which are defective in both prenylation processes,

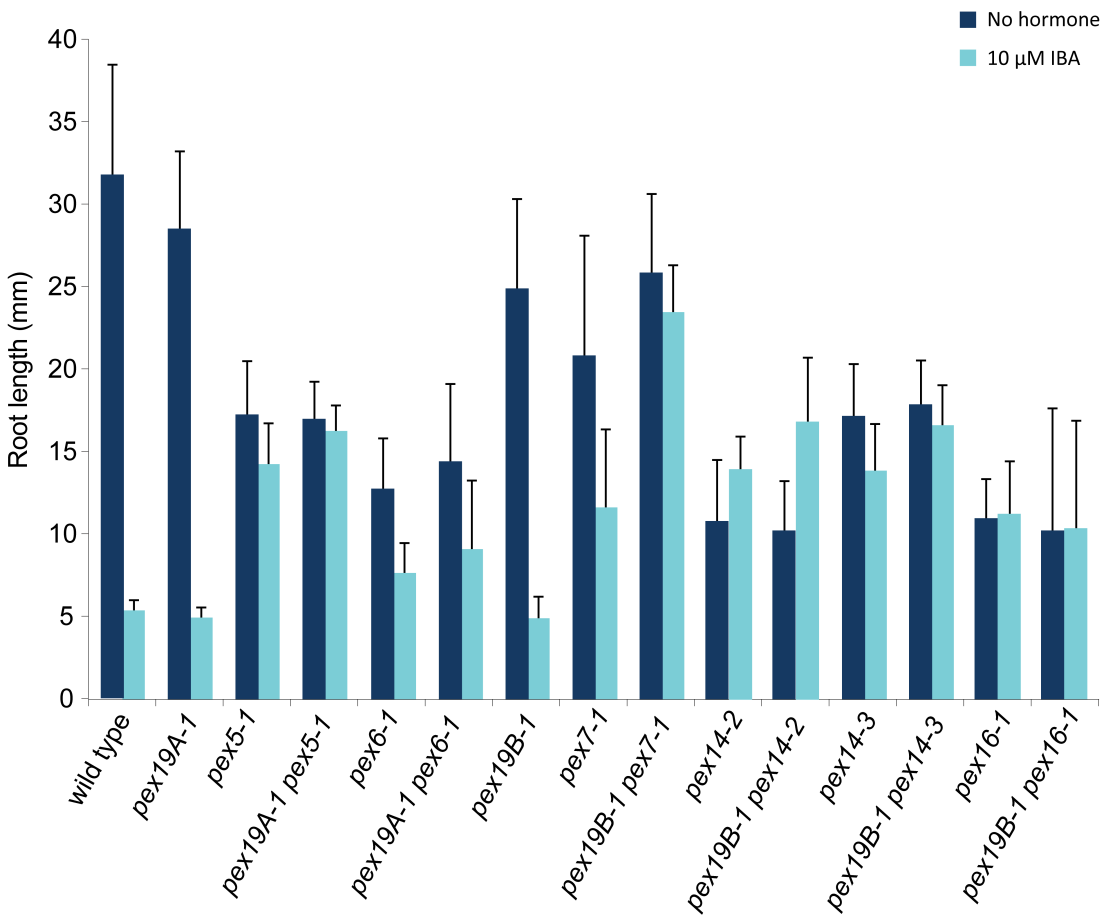

Figure 3.7. IBA response in *pex19 pex* double mutants.

Seeds were grown on medium with or without IBA under yellow-filtered light for eight days. Plants were removed and root length was measured. Bars show mean + SD; n ≥ 8. *pex19A-1* and *pex19B-1* are derived from original stock center lines and have not been backcrossed.

suggesting that targets that are normally farnesylated are instead geranylgeranylated or that the PGGT complex farnesylates targets in *era1* mutants, thereby partially rescuing farnesylation defects.

We initially hypothesized that *era1* mutants were hypersensitive to IBA because in the absence of farnesylation, PEX19 is geranylgeranylated, which renders PEX19 more functional thereby enhancing peroxisome function and IBA-to-IAA conversion. I used immunoblotting in prenylation mutants to determine if PEX19 is geranylgeranylated, in addition to being farnesylated, *in vivo*. *era1-2* is a null allele that is deficient in farnesylation (Cutler *et al*., 1996). I also isolated *ggb-2*, an insertion allele in the first exon, and *ggb-3* and *plp-3*, insertion alleles upstream of the *GGB* and *PLP* genes, respectively (Figure 3.1). Likely null alleles in *PLP* were not included in this analysis because the extreme developmental defects of these lines were incompatible with seed production in our growth conditions.

I characterized these alleles in an IBA response assay and determined that *ggb* and *plp-3* mutants responded to IBA like wild type (Figure 3.8.A). I extracted protein from the seedlings on the control plate, separated them using SDS-PAGE, and probed with various antibodies. Prenylation increases the electrophoretic mobility of PEX19 (Götte *et al.*, 1998; Matsuzono *et al.*, 1999), and I observed that PEX19 electrophoretic mobility was reduced in *era1-2* and when PEX19 lacking the CaaX domain (Col + 35S:PEX19AΔCaaX) was overexpressed (Figure 3.8.B). However, this mobility shift was not observed in *ggb* or *plp-3* mutants. Because the *plp-3* allele did not show altered PEX19 mobility, I concluded that this allele is unlikely to significantly reduce PLP

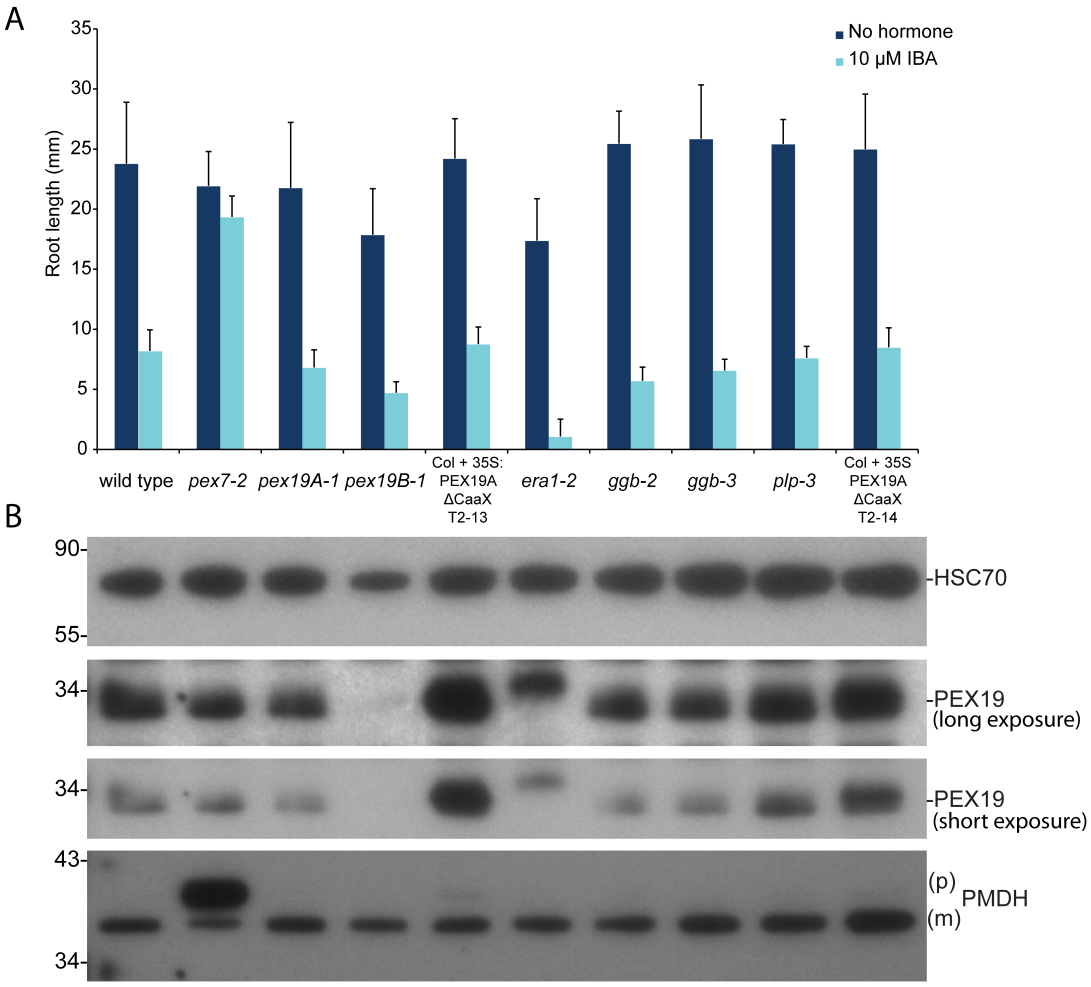

Figure 3.8. IBA response and protein accumulation in prenylation mutants.

A. Seedlings were grown on medium with or without IBA for 8 days under yellow light at 22°C . Bars show root length + SD; n ≥ 9. B. Protein was extracted from 8-10 seedlings from the "No Hormone" control plate in panel A, separated by 12% [w/v] SDS-PAGE and analyzed by immunoblotting with the indicated antibodies. *pex19A-1* and *pex19B-1* are derived from original stock center lines and have not been backcrossed. The positions of molecular weight markers are indicated on the left (in kDa). Processed PMDH is denoted by (m) for mature and unprocessed PMDH is denoted by (p) for precursor. Two exposures of α-PEX19 are shown.

levels. Because PEX19 mobility is shifted in *era1* but not *ggb* alleles, I concluded that PEX19 is farnesylated but not geranylgeranylated *in vivo*.

Because PEX19 did not appear to be prenylated in the absence of ERA1 (Figure 3.8.B), I hypothesized that PEX19 is exclusively farnesylated *in vivo*. To confirm this observation, I conducted immunoblotting on 4- and 8-day-old seedlings and included another *era1* allele (*era1-4*), which is in another genetic background (L*er*). I observed reduced electrophoretic mobility of PEX19 in both *era1-2* and *era1-4* (Figure 3.9), suggesting a complete lack of PEX19 prenylation in the absence of ERA1. In addition, PEX5, PEX7, and PEX14 protein accumulation was not altered in *pex19* or *era1* mutants in these seedlings. However, *era1-2* and *era1-4* displayed a delay in accumulation of hydroxypyruvate reductase (HPR) levels, a peroxisomal protein involved in photorespiration (Figure 3.9). This delay may reflect the slow germination of *era1* seedlings. The observation that peroxisome import (monitored by PTS2 processing; Figure 3.8B) and metabolism (monitored by IBA responsiveness; Figure 3.8.A) are not impaired in *era1* mutants, which appears to contain only PEX19 that is not prenylated (Figure 3.8.B) suggests that PEX19 prenylation is not essential for peroxisome biogenesis or function in *Arabidopsis*.

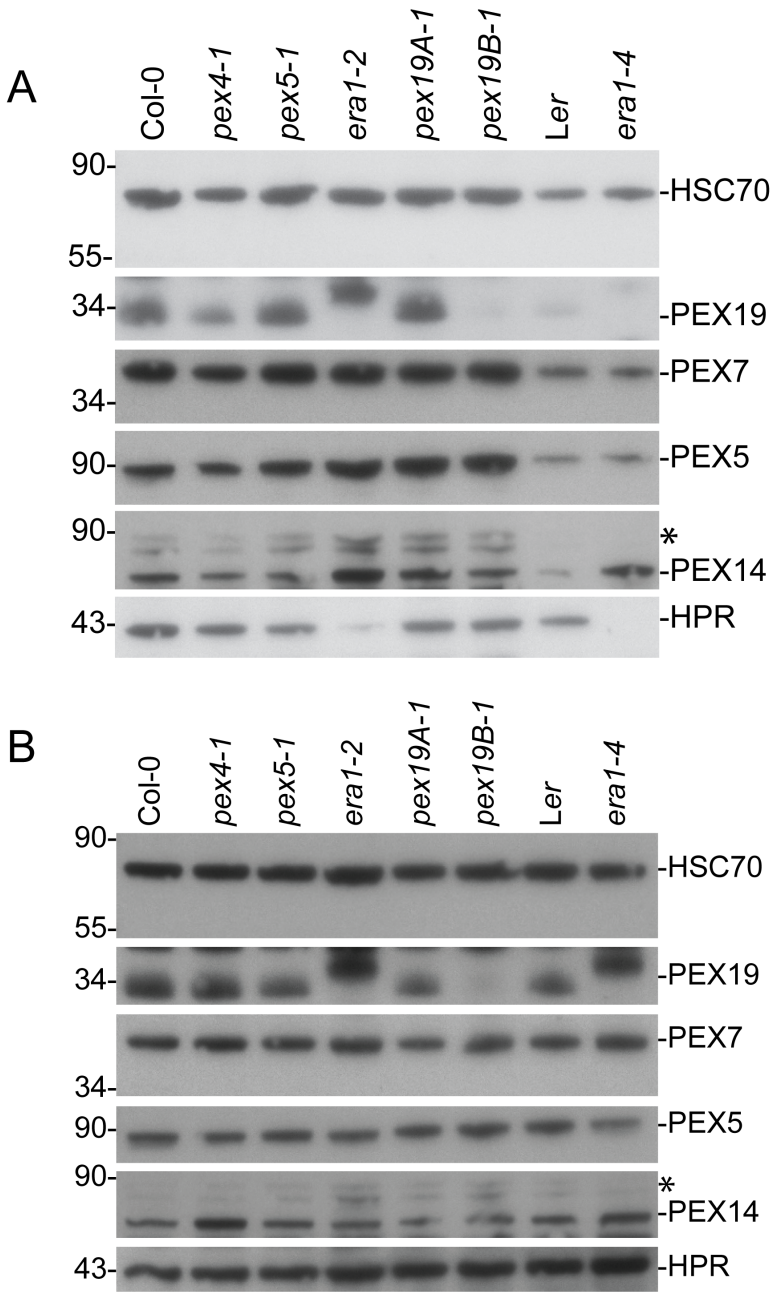

Figure 3.9. Protein accumulation in *era1* and *pex19* single mutants.

Protein accumulation in 4-day-old (A) or 8-day-old seedlings (B). Seeds were grown on sucrose-supplemented medium for 4 or 8 days under white light at 22°C. Protein from at least 8 seedlings was separated by 10% [w/v] SDS-PAGE and analyzed by western blotting with the indicated antibodies. *pex19A-1* and *pex19B-1* are derived from original stock center lines and have not been backcrossed. The positions of molecular weight markers are indicated on the left (in kDa). L*er* is the wild type control for *era1-4*; Col-0 is the wild type control for the remaining mutants. An asterisk indicates residual PEX5 and HSC70.

Chapter 4: Characterization of PEX19 overexpression lines

In yeast and mammals, the role of farnesylation on PEX19 function remains controversial (Fransen *et al.*, 2001; Vastiau *et al.*, 2006; Rucktäschel *et al.*, 2009). However, the functional significance of PEX19 farnesyaltion has not been explored in *Arabidopsis*. This chapter summarizes my work on characterizing wild type plants overexpressing various PEX19 constructs. I generated constructs in which the *PEX19A* and *PEX19B* cDNAs are driven by the 35S promoter with no epitope tag or an N-terminal YFP tag as described in Chapter 2. In addition, I created PEX19 constructs that lacked the C-terminal CaaX motif with no epitope tag or an N-terminal YFP tag. These constructs were transformed into wild type, and through these experiments, I explored the role of farnesylation in PEX19 function and localization. In the future, these lines can be crossed to the *pex19A/pex19A*; *PEX19B/pex19B* mutants to allow generation of plants in which the sole PEX19 source is from the transgene, which will allow assessment of the role of PEX19 farnesylation in *Arabidopsis*. Adrianne Stone assisted in isolating homozygous transformation lines and immunoblotting to assess expression levels.

4.1. PEX19A/B and PEX19(A/B)ΔCaaX overexpression in wild type

4.1.A. PEX19 levels and electrophoretic mobility

Arabidopsis PEX19A and PEX19B have predicted molecular weights of 28.3 kDa and 27.8 kDa, respectively. Moreover, previous reports have demonstrated that prenylation increases the electrophoretic mobility of yeast and human PEX19 (Götte *et al.*, 1998; Matsuzono *et al.*, 1999). To validate our PEX19 antibody and determine the electrophoretic mobility of *Arabidopsis* PEX19, I used various overexpression lines. I observed that PEX19 runs at an apparent molecular weight of approximately 33 kDa

(Figure 4.1). Because I could detect a new ~37 kDa protein in the lines expressing either HA-PEX19A or HA-PEX19B (Figure 4.1), I concluded that our PEX19 antibody recognizes both PEX19A and PEX19B. Furthermore, using a 12% [w/v] Bis-Tris protein gel (Invitrogen), I observed a slightly higher molecular weight band in lines overexpressing PEX19(A/B)ΔCaaX than lines overexpressing PEX19A/B (Figure 4.1), which is consistent with the observation that prenylated yeast and human PEX19 has increased electrophoretic mobility (Götte *et al.*, 1998; Matsuzono *et al.*, 1999). This result, together with my *era1* results described in Chapter 3 (Figures 3.8 and 3.9), suggests that I can distinguish between prenylated and non-prenylated PEX19. In addition, a new band of intermediate mobility is observed in the 35S:HA-PEX19 lines (Figure 4.1), suggesting that PEX19 overexpression may reduce farnesylation of endogenous PEX19.

4.1.B. PEX protein accumulation

In yeast, farnesylation enhances PEX19-PMP interactions (Rucktäschel *et al.*, 2009). Thus, I monitored accumulation of PEX14 in PEX19ΔCaaX lines to see if ectopic expression of non-farnesylated PEX19 had any dominant negative effects. Using immunoblot analysis, I observed no dramatic changes in PEX14 protein accumulation, or in accumulation of the soluble peroxins PEX5 or PEX7 (Figure 4.2).

4.1.C. PTS2 processing analysis

Mutants with impaired peroxisome matrix protein import commonly have PTS2-processing defects that can be detected by immunoblotting because PTS2-containing proteins cannot efficiently be imported into the peroxisome to have their N-terminal

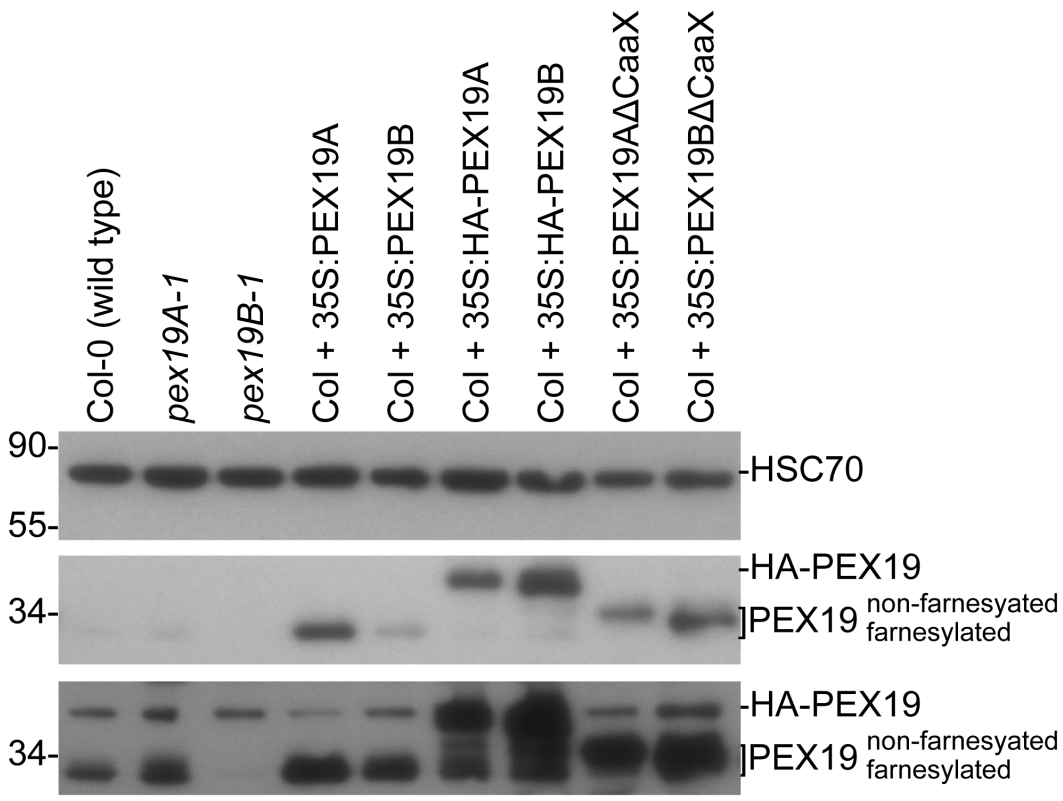

Figure 4.1. Using PEX19 overexpression lines to determine the electrophoretic mobility of PEX19.

Seedlings were grown on sucrose-supplemented medium for 8 days under white light at 22°C . Protein was extracted from 8-10 seedlings, separated by 12% [w/v] SDS-PAGE and analyzed by immunoblotting with the α-HSC70 (top) or α-PEX19 (middle and bottom; two exposures are shown) antibodies. *pex19A-1* and *pex19B-1* are derived from original stock center lines and have not been backcrossed. The positions of molecular weight markers are indicated on the left (in kDa). Expected identities of PEX19 variants are shown on the right. A cross-reacting band present at the position of HA-PEX19 is visible in the longer exposure (bottom α-PEX19 panel).

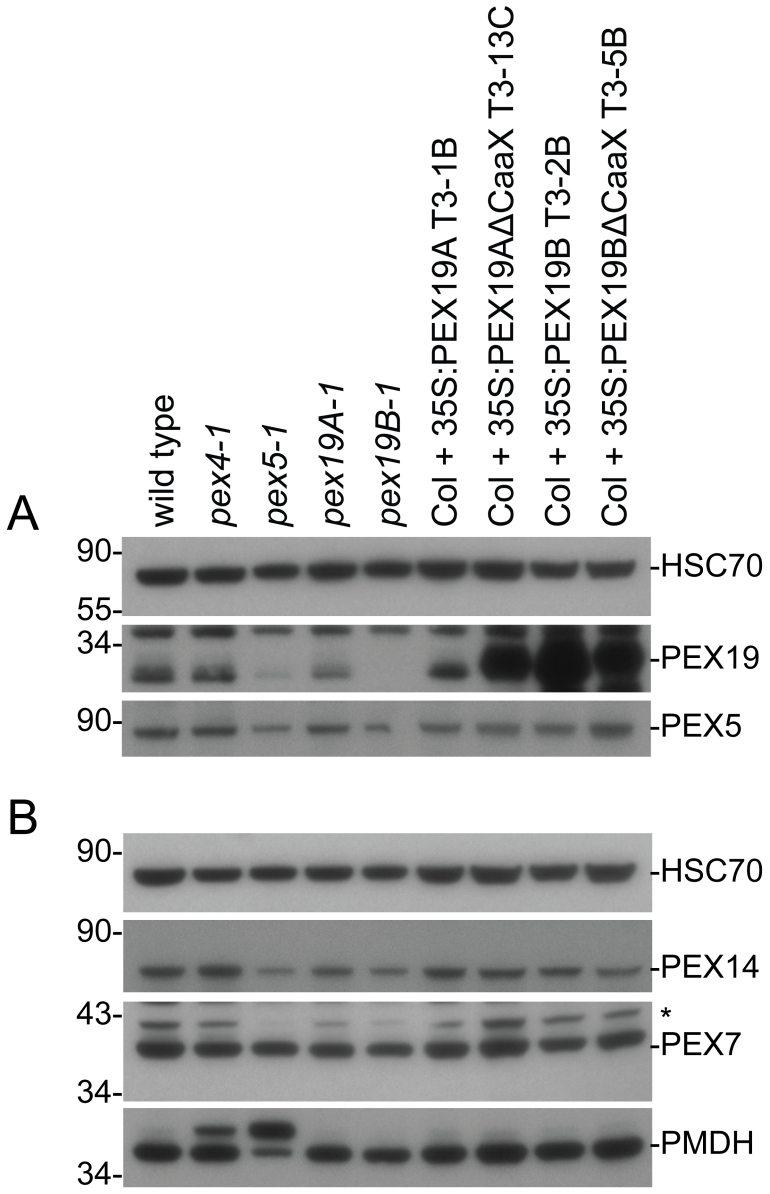

Figure 4.2. Protein accumulation in PEX19 overexpression lines.

Seedlings were grown on sucrose-supplemented medium for 8 days under white light at 22°C . Protein was extracted from 8-10 seedlings, loaded into duplicate gels, separated by 12% [w/v] SDS-PAGE and analyzed by immunoblotting with the indicated antibodies. *pex19A-1* and *pex19B-1* are derived from original stock center lines and have not been backcrossed. An asterisk indicates a cross-reacting band. The positions of molecular weight markers are indicated on the left (in kDa).

targeting sequence cleaved. Because I had seen hints of PTS2-processing defects in homozygous lines overexpressing PEX19ΔCaaX constructs in the T2 generation (Figure 3.8), I examined PTS2-processing in homozygous lines expressing PEX19 with or without the C-terminal CaaX motif by western blotting with an antibody against peroxisomal malate dehydrogenase (PMDH), a PTS2 protein. I observed that PEX19ΔCaaX did not confer a notable PTS2-processing defect (Figure 4.2).

4.1.D. Sucrose dependence and IBA response assays

To determine if overexpression of PEX19 altered any physiological phenotypes in wild-type, I conducted sucrose dependence and IBA response assays. I determined that overexpression of PEX19 with or without the C-terminal CaaX motif did not alter IBA response (Figure 4.3) or confer sucrose dependence in the dark (Figure 4.4). When I assayed sucrose dependence in the light, I observed a wide range of root lengths of both wild-type and transgenic seedlings grown in the absence of sucrose (Figure 4.5). The phenotypic heterogeneity observed within each line precludes meaningful interpretation of the data; thus, I could not form any conclusions regarding the effects of overexpressing PEX19 with or without the CaaX domain in sucrose dependence assays in the light.

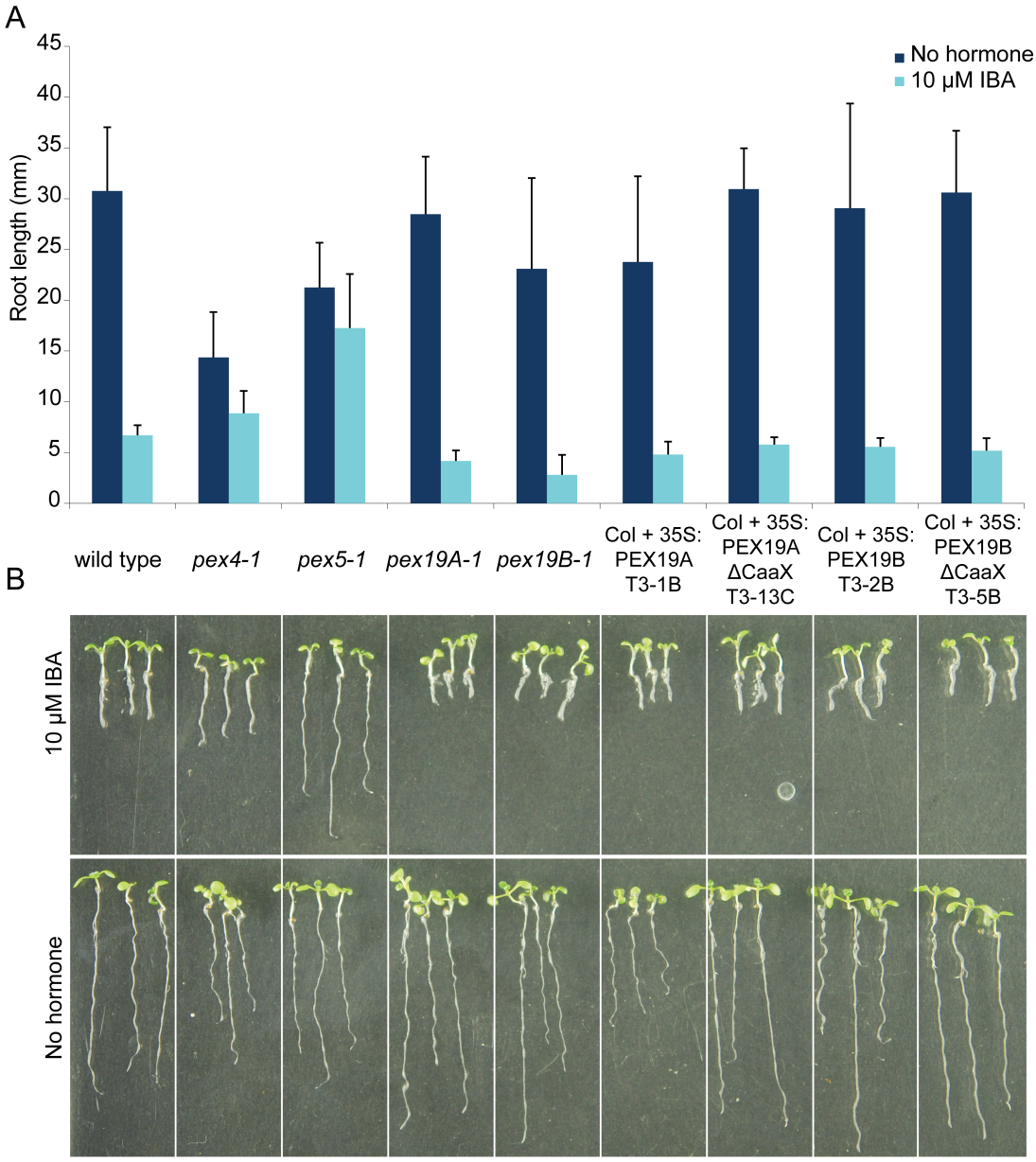

Figure 4.3. PEX19 overexpression does not alter IBA responses.

A. Root lengths of seedlings grown in the presence or absence of IBA for 8 days under yellow-filtered light. Bars show mean + SD; $n \geq 12$. B. Three seedlings representing the range of observed root lengths in panel A were arranged on a new plate and photographed. *pex19A-1* and *pex19B-1* are derived from original stock center lines and have not been backcrossed.

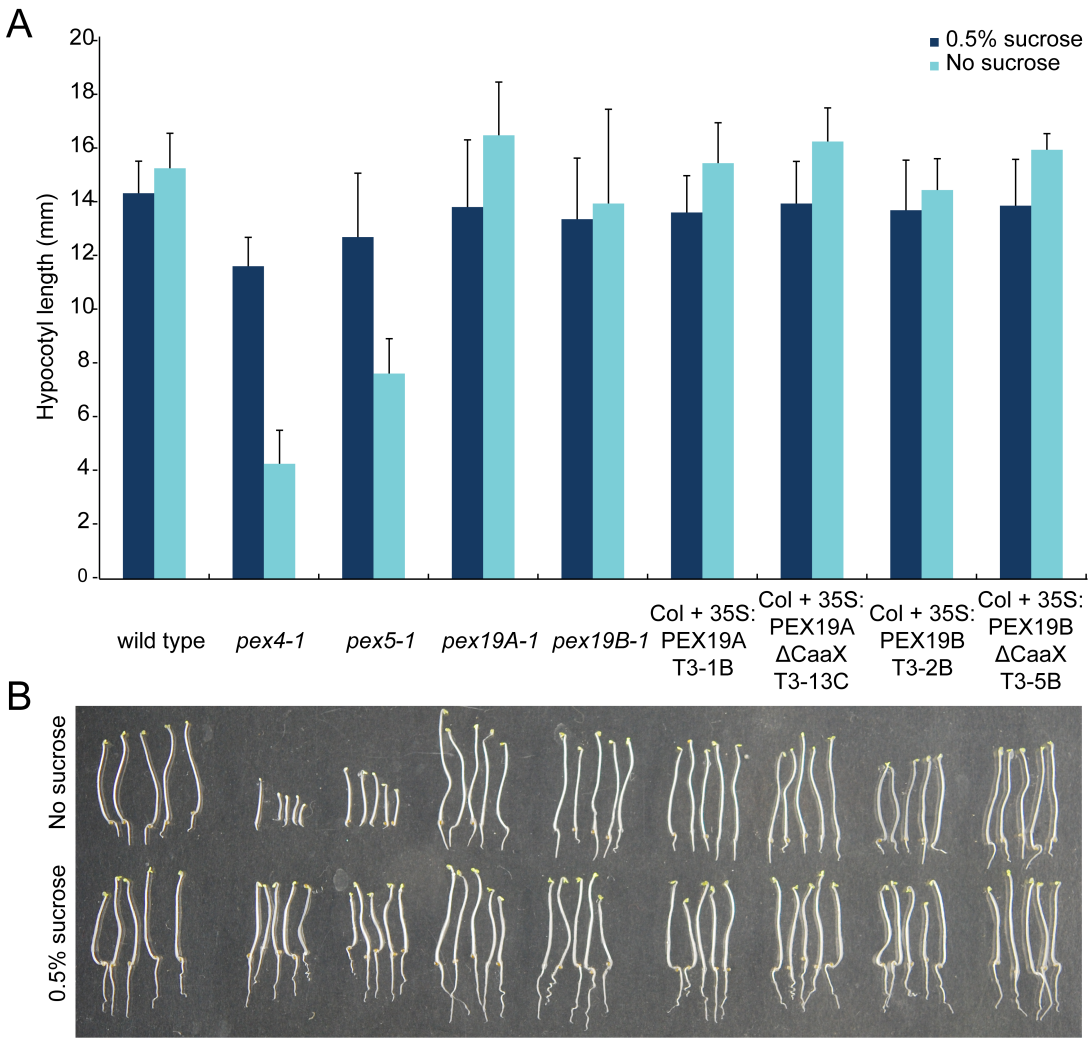

Figure 4.4. PEX19 overexpression lines are sucrose independent in the dark.

A. Hypocotyl lengths of seedlings grown in the presence or absence of 0.5% [w/v] sucrose for 1 day under white light before being transferred to the dark for another 4 days. Bars show mean + SD; $n \geq 12$. B. Five seedlings representing the range of observed root lengths in panel A were arranged on a new plate and photographed. *pex19A-1* and *pex19B-1* are derived from original stock center lines and have not been backcrossed.

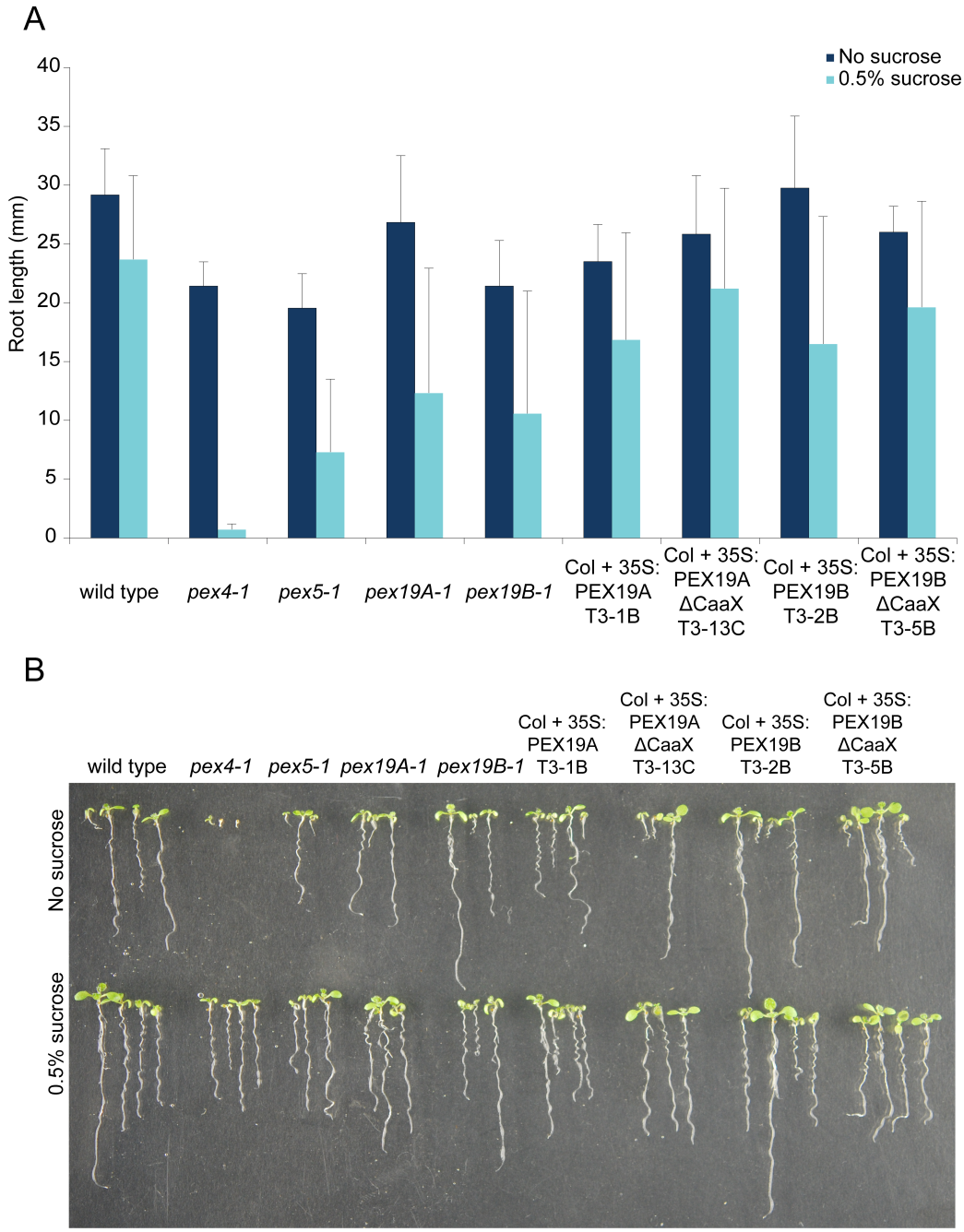

Figure 4.5. PEX19 overexpression grown with and without sucrose in the light.

A. Root lengths of seedlings grown in the presence or absence 0.5% [w/v] sucrose for 8 days under white light. Bars show mean + SD; $n \geq 12$. B. Seedlings representing the range of observed root lengths in panel A were arranged on a new plate and photographed. *pex19A-1* and *pex19B-1* are derived from original stock center lines and have not been backcrossed.

4.2. PEX19A/B and PEX19(A/B)ΔCaaX localization studies using YFP

PEX19 has been reported to be bimodally distributed between the cytosol and peroxisome in mammals (Sacksteder *et al*., 2000) and yeast (Götte *et al.*, 1998). However, PEX19 subcellular localization has not been explored in *Arabidopsis*.

4.2.A. Microscopy

To begin to examine the subcellular localization of farnesylated and non-farnesylated PEX19A and PEX19B, I transformed wild type plants with a construct overexpressing YFP-PEX19 fusion proteins under the control of the 35S promoter. I used a wild-type line overexpressing yellow fluorescent protein with a C-terminal peroxisomal targeting sequence (YFP-SKL) (*Arabidopsis* stock center number CS16261; Nelson *et al*., 2007) as a positive control and segregating YFP-PEX19 T2 lines for confocal microscopy.

I observed that peroxisomally-targeted YFP was distributed in a punctate pattern that indicated peroxisome localization in cells of cotyledons, hypocotyls, and roots (Figure 4.6; YFP-SKL). However, YFP-PEX19 fusion proteins appeared to be more diffuse and mostly localized to the cytosol and/or a subcellular membrane. Interestingly, YFP-PEX19BΔCaaX was not expressed or did not accumulate in the root, even though all constructs were driven by the same viral promoter (CaMV 35S). However, I did not detect localization alterations of the YFP-PEX19 with or without the CaaX motif in cotyledon or hypocotyl cells (Figure 4.6) This result is consistent with the possibility that farnesylation does not impact PEX19 localization, but it is also possible that the high expression level of these constructs has impacted protein targeting.

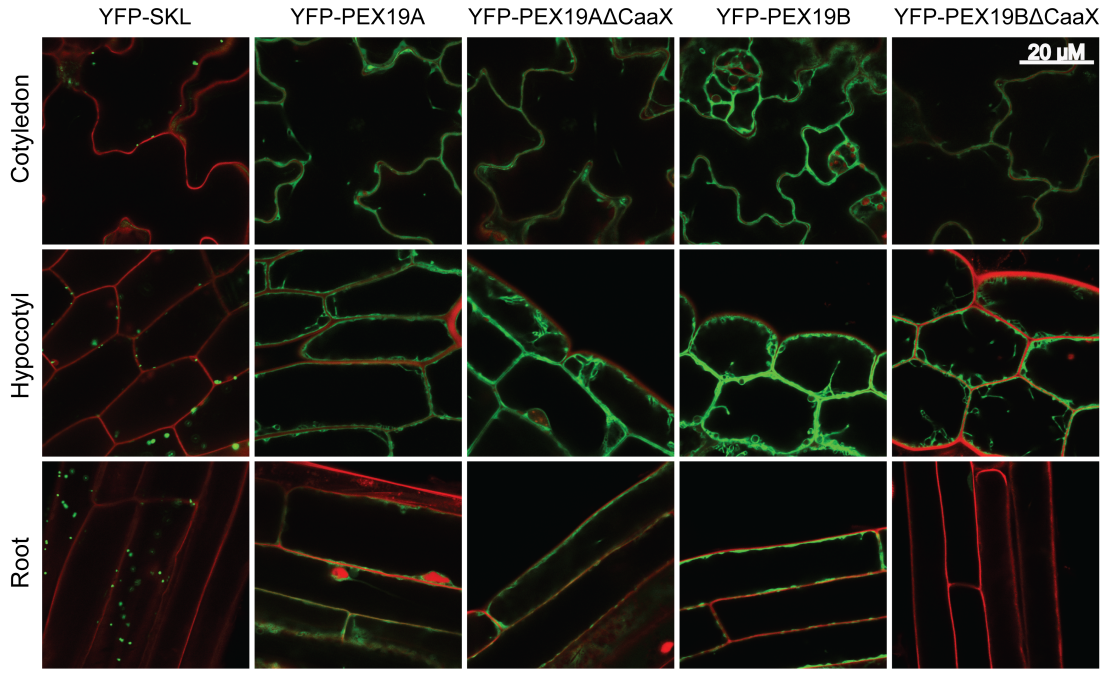

Figure 4.6. PEX19A/B and PEX19(A/B)ΔCaaX localization using yellow fluorescent protein.

Seedlings were grown on sucrose-supplemented medium for 6 days under white light before being analyzed using confocal fluorescence microscopy. As a positive control peroxisomally-targeted YFP was overexpressed in wild type and visualized (far left panel; green). YFP was fused to the N-terminus of PEX19 and overexpressed in wild type to determine PEX19 localization patterns (green). Seedlings were stained with propidium iodide, which stains cell walls (red), for approximately 30 minutes before visualization. Due to the presence of a large central vacuole, most of the cytosol is at the cell margins.

4.2.B. YFP-PEX19 levels

I used immunoblot analysis to verify that the lines used in the YFP-PEX19 localization studies were expressing a YFP-PEX19 fusion protein. By using antibodies to either PEX19 or GFP, I detected a ~55 kDa protein (Figure 4.7), which is the predicted molecular weight for the YFP-PEX19 fusion proteins. Furthermore, in the control (Col + 35S:YFP-SKL) I detected a ~27 kDa protein (Figure 4.7), which is the predicted molecular weight of YFP. Although the α-GFP antibody detects some degradation products of the YFP-PEX19 fusion proteins, most of the YFP-PEX19 appears to be intact in these lines (Figure 4.7), suggesting that the bulk of the fluorescence observed in Figure 4.6 was due to YFP-PEX19 and not proteolytic fragments of the fusion protein.

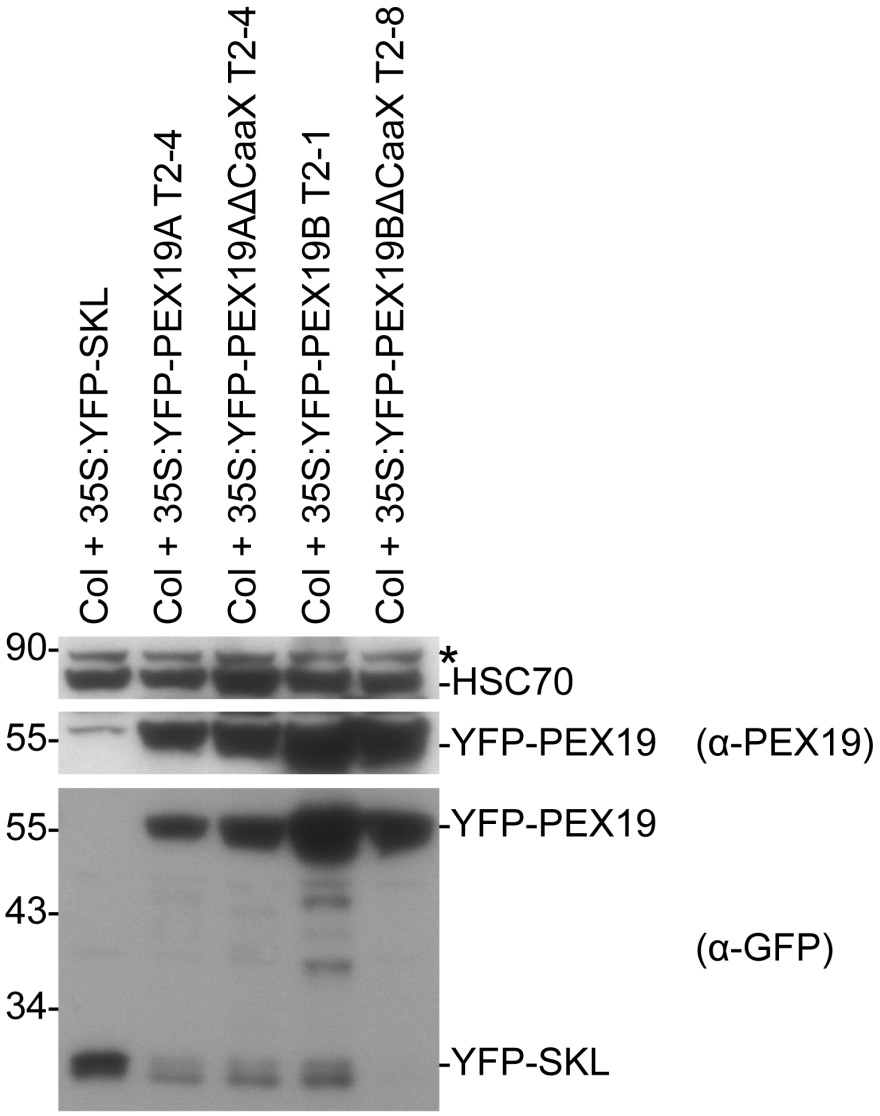

Figure 4.7. Immunoblot to confirm YFP-PEX19 expression.

Siblings from individuals used for confocal microscopy (Figure 4.5) were grown on PNS for 6 days and pooled. Protein was extracted and separated by 12% [w/v] SDS-PAGE and analyzed by immunoblotting with the indicated antibodies. An asterisk denotes a cross-reacting band from the PEX19 antibody. The positions of molecular weight markers are indicated on the left (in kDa).

Chapter 5: Discussion and future directions

5.1. The role of PEX19 in *Arabidopsis*

PEX19 is a farnesylated protein that is thought to function as a cytosolic receptor for PMPs in yeast (Otzen *et al*., 2004; Rottensteiner *et al*., 2004; Halbach *et al*., 2006) and mammals (Sacksteder *et al*., 2000; Jones *et al*., 2004). In *Saccharomyces cerevisiae,* PEX19 is essential for the production of pre-peroxisomes from the endoplasmic reticulum (Hoepfner *et al.*, 2005). Furthermore, yeast *pex19* mutants do not make peroxisomes (reviewed by Schliebs and Kunau, 2004), and PEX19 is required for peroxisome membrane assembly in Chinese hamster ovary cells (Matsuzono *et al*., 1999). In *Arabidopsis*, *pex19* RNAi knockdown lines have reduced matrix protein import and enlarged peroxisomes (Nito *et al*., 2007).

Because PEX19 plays an integral role in peroxisome biogenesis in yeast and mammals, I was surprised to observe no obvious physiological defects in *pex19* T-line single mutants in IBA response (Figures 3.2 and 3.3) or sucrose dependence (Figure 3.4) assays. However, after crossing the *pex19* single mutants to each other, plating F3 individuals on 10 μM IBA, and genotyping individuals, I observed that *pex19B* single mutants were IBA resistant (Figure 3.5). This result suggests that there may be a suppressor mutation in the *pex19B* T-line that segregated out after crossing the *pex19* single mutants to each other. We have backcrossed the *pex19A* and *pex19B* T-lines to wild type, and these lines will need to be characterized in physiological assays to assess peroxisome function in the *pex19* single mutants.

Moreover, I screened through 108 F2 individuals from the *pex19A pex19B* cross and did not recover a double mutant, suggesting that the double mutant is inviable. Thus, it

appears that PEX19 is likely essential for embryogenesis. Indeed, other peroxin mutants, including nulle alleles of *PEX2*, *PEX10*, and *PEX12*, confer embryonic lethality (Lin *et al*., 1999; Hu *et al*., 2002; Schuhmann *et al*., 2003; Sparkes *et al*., 2003; Fan *et al*., 2005).

I found that 8-day-old *pex19B* T-line seedlings had reduced accumulation of PEX19 (Figure 3.8), whereas *pex19A* T-line seedlings had normal PEX19 levels (Figure 3.8), suggesting that PEX19B is more abundant than PEX19A in 8-day-old seedlings. Because the *pex19B* T-lines did not have any obvious peroxisomal defects in physiological assays (Figures 3.2, 3.3, and 3.4), I tested whether PEX19A was more abundant in younger seedlings by conducting western blots with 3-, 5-, and 8-day-old seedlings. I found that at all three time points *pex19B* mutants accumulated very little PEX19 (Figure 3.6). Despite the apparent lack of PEX19, *pex19B* seedlings had normal levels of PEX5, PEX7, and PEX14 and no PTS2-processing defect (Figure 3.6). However, it would be interesting to examine levels of additional PMPs in *pex19* mutants, as I only examined PEX14, which is not dramatically altered in yeast *pex19* mutants (Rucktäschel *et al.*, 2009). Collectively, these data suggest that seedling peroxisome function only requires a small amount of PEX19. It would be interesting to assess PEX19 levels in these mutants during embryogenesis and very early seedling development.

In addition, it was observed that *pex19A* did not appear to alter IBA response in *pex5-1* or *pex6-1* mutants (Figure 3.7; Adrianne Stone, personal communication). However, *pex19B* noticeably enhanced the IBA resistance of *pex7-1* (Figure 3.7; Adrianne Stone, personal communication). This enhancement suggests that peroxisome function is compromised in *pex19B* and is consistent with the observation that *pex19B* is IBA resistant in some genetic backgrounds whereas *pex19A* is not (Figure 3.5). It will be

interesting to assess sucrose dependence and protein accumulation in these and more *pex19 pex* double mutants.

5.2. The prenylation state of PEX19 in *Arabidopsis*

PEX19 is farnesylated in yeast (Götte *et al.*, 1998; Rucktäschel *et al.*, 2009) and mammals (James *et al*., 1994; Sacksteder *et al*., 2000; Mayerhofer *et al.*, 2002; Vastiau *et al.*, 2006). Before this work, prenylation of *Arabidopsis* PEX19 had not been demonstrated *in vivo*, but the conserved C-terminal CaaM motif suggested that PEX19 proteins are farnesylated *in vivo*. Because protein farnesyltransferase and geranylgeranyltransferase substrate promiscuity exists, proteins with certain permutations of a CXXM motif can be geranylgeranylated *in vitro* (Andrews *et al.*, 2010). However, it was not known if proteins bearing a CCIM or CCVM motif found on *Arabidopsis* PEX19 can be geranylgeranylated.

To further explore the role of prenylation in PEX19 and peroxisome function, I isolated *ggb-2*, *ggb-3*, and *plp-3* insertion alleles (Figure 3.1). Prenylation mutants were characterized in an IBA response assay, and I found that *ggb* and *plp* mutants responded to IBA like wild type and *era1-2* is hypersensitive to IBA (Figure 3.8.A). I observed that PEX19 electrophoretic mobility was reduced in *era1-2* but not *ggb* or *plp-3* (Figure 3.8.B). The *plp-3* allele contains a T-DNA insertion 5' of the *PLP* transcription start site. Because the *plp-3* allele does not alter the electrophoretic mobility of PEX19, I concluded that this mutant probably does not have sufficiently reduced PLP levels to impact farnesylation and is not a useful mutant for this analysis. Because prenylation increases the electrophoretic mobility of PEX19 (Götte *et al.*, 1998; Matsuzono *et al*., 1999), the PEX19 molecular weight shift in *era1-2* suggests that PEX19 is not prenylated in the

absence of ERA1. I observed a slight difference in electrophoretic mobility between PEX19AΔCaaX and PEX19 in *era1-2* (Figure 3.8). This difference may result from the four terminal amino acids being deleted in the lines overexpressing PEX19AΔCaaX, whereas full-length PEX19 is predicted to be present in *era1-2*.

Because PEX19 did not appear to be prenylated in *era1-2* (Figure 3.8.B) or *era1-4* (Figure 3.9), I concluded that PEX19 is exclusively or predominantly farnesylated *in vivo*. Alternatively, a small amount of PEX19 may be geranylgeranylated but is not detectable in these experiments. Furthermore, the lack of prenylated PEX19 in *era1* mutants did not appear impede PTS2 processing (Figure 3.8.B), decrease IBA responses (Figure 3.8.A), or alter PEX5, PEX7, or PEX14 levels in 4- or 8-day-old seedlings (Figure 3.9). This result suggests that if PEX19 is needed for peroxisome biogenesis in *Arabidopsis*, prenylation of PEX19 is not essential for this function.

This study was motivated by the observation that *era1* displays enhanced IBA responsiveness, but my western analyses do not support our original hypothesis that PEX19 might be geranylgeranylated in the absence of farnesylation, leading to a hyperactive protein. What is then the cause of the increased IBA sensitivity phenotype of *era1*?

5.3. The apparent IBA hypersensitivity of *era1-2* may be explained by delayed development

In oilseed plants, such as *Arabidopsis*, peroxisomes are essential during seedling germination and establishment because stored fatty acids are β-oxidized and converted to sugar via the glyoxylate cycle, which is housed in specialized peroxisomes called glyoxysomes (reviewed by Graham, 2008). After germination and development of

photosynthetic abilities, seedlings remodel their enzymatic composition in the peroxisome and transition from a glyoxysome to a leaf-type peroxisome (reviewed by Michels *et al*., 2005). During this transition, the genes encoding enzymes in the glyoxylate cycle, such as isocitrate lyase (ICL) and malate synthase (MLS) are downregulated, and genes encoding enzymes necessary for photorespiration, such as hydroxypyruvate reductase (HPR), are upregulated (Lingard *et al*., 2009). HPR is first detectable at 4 days in wild type. However, I found that *era1* mutants had reduced HPR accumulation at 4 days compared to wild type (Figure 3.9.A). Because *era1* is a pleiotropic mutant and has an enhanced response to abscisic acid (ABA), which inhibits germination, these results suggest that the apparent *era1* hypersensitivity to IBA (Figure 3.8) that motivated these studies may result from a delayed transition from glyoxysomes, which specialize in β-oxidation, to leaf-type peroxisomes, which specialize in photorespiration, rather than from enhanced peroxisome function or activity.

5.4. Farnesylation does not alter accumulation of a subset of peroxins or confer dominant negative phenotypes.

The role of farnesylation in PEX19 function remains controversial in yeast and mammals (Fransen *et al.*, 2001; Vastiau *et al.*, 2006; Rucktäschel *et al.*, 2009). To assess the functional significance of farnesylation in *Arabidopsis* PEX19 function, I created *PEX19A* and *PEX19B* cDNA overexpression constructs that produce full-length and truncated PEX19 that lacks the C-terminal CaaX motif. Wild-type plants were transformed with these constructs, and homozygous lines were isolated and characterized. I determined that overexpression of PEX19 with or without the C-terminal CaaX motif did not alter PEX5, PEX7, or PEX14 protein accumulation (Figure 4.2), alter the wild

type response to IBA (Figure 4.3) or render sucrose dependence in the dark (Figure 4.4), suggesting that these constructs do not confer dominant negative phenotypes. To determine if farnesylation is essential for PEX19 function, these constructs could be crossed into the *PEX19A/pex19A*;*pex19B/pex19B* mutants to determine if constructs expressing PEX19 with and without the CaaX motif rescue the lethality of the *pex19* double mutant.

Farnesylation is suggested to alter PEX19-PMP interactions. For example, in *S. cerevisiae*, farnesylation is required for the stability of a subset of PMPs, including the RING finger complex comprised of PEX2, PEX10, and PEX12, and the peroxisome proliferation protein, PEX11 (Rucktäschel *et al.*, 2009); however, farnesylation is not required for the stability of the docking complex PMPs, PEX13 and PEX14 (Rucktäschel *et al.*, 2009). Furthermore, farnesylation of PEX19 increases the binding affinity of yeast PEX19 for a variety of PMPs, including PEX11, PEX12, and PEX13 (Rucktäschel *et al.*, 2009). Thus, *Arabidopsis* PEX19 may be functional in the absence of a farnesyl group but may have a reduced affinity for some PMPs. To further investigate this possibility, coimmunoprecipitation experiments could be conducted using pull-downs with extracts from wild type overexpressing YFP-PEX19 fusion proteins with and without the CaaX motif followed by immunoblot analysis to assess PMP levels and determine if farnesylation alters PEX19-PMP interactions.

In addition, I have created constructs overexpressing PEX19 with the terminal amino acid (Met) changed to leucine (PEX19-CaaL). Because of the CaaL motif, PEX19 will presumably be preferentially geranylgeranylated *in vivo,* and this modification may alter electrophoretic mobility so that it can be distinguished from farnesylation in a

western blot. It will be interesting to determine if geranylgeranylated PEX19 alters PEX19 function and/or PEX19-PMP interactions using assays that assess peroxisome activity (i.e., rescue of the *pex19A pex19B* lethality) and coimmunoprecipitations.

5.5. YFP-PEX19 is associated with subcellular membranes and farnesylation is not required for proper localization.

PEX19 is predominantly cytosolic and partially associated with the peroxisome membrane in yeast (Götte *et al.*, 1998) and mammals (Sacksteder *et al*., 2000). However, the subcellular localization of PEX19 had not been examined in *Arabidopsis* until this study. I created constructs expressing YFP-PEX19 fusion proteins with and without the C-terminal CaaX motif and used confocal fluorescence microscopy to observe that YFP-PEX19A/B appeared to be associated with a subcellular membrane, perhaps the ER, in all tissues examined (Figure 4.6). Deletion of the C-terminal CaaX domain did not noticeably alter YFP-PEX19 subcellular distribution (Figure 4.6); however, I observed very little YFP-PEX19BΔCaaX expression/accumulation root tissue (Figure 4.6), which suggests that farnesylation may be required for PEX19B accumulation in roots. However, reduced YFP-PEX19BΔCaaX expression may be due to an abberant genome insertion. For example, in plants transgenes are susceptible to a variety of transcriptional and post-transcriptional gene-silencing mechanisms that may be a result of the epigenetic regulation of the locus in which the transgene inserted (reviewed by Vaucheret *et al*., 1998). To eliminate the possibility of transgene silencing, more lines from independent insertion events will need to be examined. In addition, it would be interesting to examine PEX19 accumulation in roots versus shoots of the *era1* mutants, which accumulates non-farnesylated PEX19.

To determine if YFP-PEX19 is localized to the ER, YFP-PEX19 lines with and without the CaaX motif could be crossed to a line carrying transgenes encoding fluorescence markers for the ER and peroxisomes (Nelson *et al*., 2007) and used to conduct co-localization studies. Furthermore, it will be interesting to determine if geranylgeranylation of PEX19 alters subcellular localization. For these studies, I have created constructs expressing PEX19-CaaL with an N-terminal YFP epitope tag. Presumably YFP-PEX19-CaaL will be preferentially geranylgeranylated, and confocal fluorescent microscopy could be used to assess the cellular distribution of YFP-PEX19-CaaL. Additionally, to determine if these YFP-PEX19 fusion proteins are functional, these constructs will need to rescue the inviability of the *pex19A pex19B* double mutant.

5.6. Summary and conclusions

In summary, I determined that *pex19B* has reduced PEX19 protein accumulation in young seedlings (Figure 3.6) but surprisingly did not have altered PEX5/7/14 levels (Figure 3.6), PTS2-processing defects (Figure 3.6), or impaired peroxisome function (Figures 3.2, 3.3, and 3.4). However, I am baffled by the observation that *pex19B* mutants were IBA resistant when isolated from cross progeny (Figure 3.5). I also observed that reduced PEX19B enhances the IBA resistance of *pex7-1* but not *pex14* or *pex16-1* mutants (Figure 3.7). Additionally, I used prenylation mutants to determine that PEX19 is predominantly, if not exclusively, farnesylated *in vivo* (Figures 3.8 and 3.9) and farnesylation is not essential for peroxisome function (Figure 3.8). Also, the apparent IBA hypersensitvity phenotype of *era1* (Figure 3.8) is likely due to delayed development and transition from a glyoxysome to a transitional peroxisome (Figure 3.9).

I also characterized PEX19 overexpression lines and observed that PEX19 overexpression did not alter PEX5/7/14 accumulation (Figure 4.2) or wild type response to IBA (Figure 4.3) or confer sucrose dependence (Figures 4.4 and 4.5). Lastly, using YFP-PEX19 fusion proteins, I determined that YFP-PEX19 localizes to a subcellular membrane that appears to be the ER and farnesylation was not required for this localization.

5.7. Final thoughts

Although peroxisome matrix protein import has been relatively well characterized, the exploration of peroxisome biogenesis and PMP import and membrane assembly is still in its infancy. I have determined that PEX19 is largely farnesylated *in vivo* in *Arabidopsis* and developed the tools to determine whether this farnesylation contributes to PEX19 function *in vivo*.

References

Alonso, J.M., Stepanova, A.N., Leisse, T.J., Kim, C.J., Chen, H., Shinn, P., Stevenson, D.K., Zimmerman, J., Barajas, P., Cheuk, R., Gadrinab, C., Heller, C., Jeske, A., Koesema, E., Meyers, C.C., Parker, H., Prednis, L., Ansari, Y., Choy, N., Deen, H., Geralt, M., Hazari, N., Hom, E., Karnes, M., Mulholland, C., Ndubaku, R., Schmidt, I., Guzman, P., Aguilar-Henonin, L., Schmid, M., Weigel, D., Carter, D.E., Marchand, T., Risseeuw, E., Brogden, D., Zeko, A., Crosby, W.L., Berry, C.C., and Ecker, J.R. 2003. Genome-wide insertional mutagenesis of *Arabidopsis thaliana*. Science *301*:653-657.

Andrews, M., Huizinga, D.H., and Crowell, D.N. 2010. The CaaX specificities of *Arabidopsis* protein prenyltransferases explain *era1* and *ggb* phenotypes. BMC Plant Biol. *10*:118

Ausubel, F.M., Katagiri, F., Mindrinos, M., and Glazebrook, J. 1995. Use of *Arabidopsis thaliana* defense-related mutants to dissect the plant response to pathogens. PNAS *92*:4189-96.

Ausubel, F., Brent, R., Kingston, R.E., Moore, D.D., Seidman, J.G., Smith, J.A., and Struhl, K. 1999. Current Protocols in Molecular Biology (New York: Greene Publishing Associates and Wiley-Interscience).

Bonetta, D., Bayliss, P., Sun, S., Sage, T., McCourt, P. 2000. Farnesylation is involved in meristem organization in *Arabidopsis*. Planta *211*:182-90.

Brown, L.A. and Baker, A. 2008. Shuttles and cycles: transport of proteins into the peroxisome matrix. Mol. Membr. Biol. *25*:363-75.

Celenza, J.L. Jr., Grisafi, P.L., and Fink, G.R. 1995. A pathway for lateral root formation in *Arabidopsis thaliana*. Genes Dev. *9*:2131-42.

Clough, S.J. and Bent, A.F. 1998. Floral dip: a simplified method for *Agrobacterium*-mediated transformation of *Arabidopsis thaliana*. Plant J. *16*:735-43.

Crowell, D.N. 2000. Functional implications of protein isoprenylation in plants. Prog. Lipid Res. *39*:393-408.

Cutler, S., Ghassemian, M., Bonetta, D., Cooney, S., and McCourt, P. 1996. A protein farnesyl transferase involved in abscisic acid signal transduction in *Arabidopsis*. Science *273*:1239-1241

Earley, K., Haag, J., Pontes, O., Opper, K., Juehne, T., Song, K., and Pikaard, C. 2006. Gateway-compatible vectors for plant functional genomics and proteomics. Plant J. *45*:616-629.

Fan, J., Quan, S., Orth, T., Awai, C., Chory, J., and Hu, J. 2005.The *Arabidopsis* PEX12 gene is required for peroxisome biogenesis and is essential for development. Plant Physiol. *139*:231-9.

Fang, Y., Morell, J.C., Jones, J.M., and Gould, S.J. 2004. PEX3 functions as a PEX19 docking factor in the import of class I peroxisomal membrane proteins. J. Cell Biol. *164*:863-875.

Fagarasanu, A., Fagarasanu, M., and Rachubinski, R.A. 2007. Maintaining peroxisome populations: a story of division and inheritance. Annu. Rev. Cell Dev. Biol. *23*:321-344.

Fransen, M., Wylin, T., Brees, C., Mannaerts, G.P., and Van Veldhoven, P.P. 2001. Human Pex19p binds peroxisomal integral membrane proteins at regions distinct from their sorting sequences. Mol. Cell Biol. *21*:4413-24.

Fujiki, Y., Matsuzono, Y., Matsuzaki, T., and Fransen, M. 2006. Import of peroxisomal membrane proteins: the interplay of Pex3p- and Pex19p-mediated interactions. Biochim. Biophys. Acta. *1763*:1639-46.

Götte, K., Girzalsky, W., Linkert, M., Baumgart, E., Kammerer, S., Kunau, W., and Erdmann, R. 1998. Pex19p, a farnesylated protein essential for peroxisome biogenesis. Mol. Cell Biol. *18*:616-628.

Graham, I. 2008. Seed storage oil mobilization. Annu. Rev. Plant Biol. *59*:115-42.

Hadden, D.A., Phillipson, B.A. Johnston, K.A., Brown, L.-A., Manfield, I.W., El-Shami, M., Sparkes, I.A., and Baker, A. 2006. *Arabidopsis* PEX19 is a dimeric protein that binds the peroxin PEX10. Mol. Membr. Biol. *23*:325-336.

Halbach, A., Landgraf, C., Lorenzen, S., Rosenkranz, K., Volkmer-Engert, R., Erdmann, R., and Rottensteiner, H. 2006. Targeting of the tail-anchored peroxisomal membrane proteins PEX26 and PEX15 occurs through C-terminal PEX19-binding sites. J. Cell Sci. *119*:2508-17.

Haughn, G.W., and Somerville, C. 1986. Sulfonylurea-resistant mutants of *Arabidopsis thaliana*. Mol. Gen. Genet. *204*:430-4.

Hayashi, M., Toriyama, K., Kondo, M., and Nishimura, M. 1998. 2,4-Dichlorophenoxybutyric acid-resistant mutants of *Arabidopsis* have defects in glyoxysomal fatty acid β-oxidation. Plant Cell *10*:183-195.

Hayashi, M. and Nishimura, M. 2003. Entering a new era of research on plant peroxisomes. Curr. Opin. Plant Biol. *6*:577-82.

Helm, M., Lück, C., Prestele, J., Hierl, G., Huesgen, P.F., Frölich, T., Arnold, G.J., Adamska, I., Görg, A., Lottspeich, F., and Gietl, C. 2007. Dual specificities of the glyoxysomal/peroxisomal processing protease Deg15 in higher plants. PNAS *104*:11501-11506.

Hoepfner, D., Schildknegt, D., Braakman, I., Philippsen, P., and Tabak, H.F. 2005. Contribution of the endoplasmic reticulum to peroxisome formation. Cell *122*:85-95.

Hu, J., Aguirre, M., Peto, C., Alonso, J., Ecker, J., and Chory, J. 2002. A role for peroxisomes in photomorphogenesis and development in *Arabidopsis*. Science *297*:405-9.

James, G.L., Goldstein, J.L., Pathak, R.K., Anderson, R.G., and Brown, M.S. 1994. PxF, a prenylated protein of peroxisomes. J. Biol. Chem. *269*:14182-14190.

Jones, J.M., Morell, J.C., and Gould, S.J. 2004. PEX19 is a predominantly cytosolic chaperone and import receptor for class 1 peroxisomal membrane proteins. J. Cell Biol. *164*:57-67.

Kleczkowski, L.A. and Randall, D.D. 1988. Purification and characterization of a novel NADPH(NADH)-dependent hydroxypyruvate reductase from spinach leaves. Comparison of immunological properties of leaf hydroxypyruvate reductases. Biochem. J. *250*:145-52.

Koncz, C., Németh, K., Rédei, G., and Schell, J. 1992. T-DNA insertional mutagenesis in *Arabidopsis*. Plant Mol. Biol. *20*:963-76.

Lanyon-Hogg, T., Warriner, S.L., and Baker, A. 2010. Getting a camel through the eye of a needle: the import of folded proteins by peroxisomes. Biol. Cell *102*:245-63.

Last, R.L. and Fink, G.R. 1988. Tryptophan-requiring mutants of the plant *Arabidopsis thaliana*. Science *240*:305-10.

Lin, Y., Sun, L., Nguyen, L.V., Rachubinski, R.A., and Goodman, H.M. 1999. The Pex16p homolog SSE1 and storage organelle formation in *Arabidopsis* seeds. Science *284*:328-30.

Lingard, M.J. and Bartel, B. 2009. *Arabidopsis* LON2 is necessary for peroxisomal function and sustained matrix protein import. Plant Phys. *151*:1354-1365.

Lingard, M.J., Monroe-Augustus, M., and Bartel, B. 2009. Peroxisome-associated matrix protein degradation in *Arabidopsis*. PNAS *106*:4561-4566.

Ma, C., Agrawal, G., and Subramani, S. 2011. Peroxisome assembly: matrix and membrane protein biogenesis. J. Cell Biol. *193*:7-16.

Matsuzono, Y., Kinoshita, N., Tamura, S., Shimozawa, N., Hamasaki, M., Ghaedi, K., Wanders, R.J., Suzuki, Y., Kondo, N., and Fujiki, Y. 1999. Human PEX19: cDNA cloning by functional complementation, mutation analysis in a patient with Zellweger syndrome, and potential role in peroxisomal membrane assembly. PNAS *96*:2116-21.

Matsuzono, Y. and Fujiki, Y. 2006. *In vitro* transport of membrane proteins to peroxisomes by shuttling receptor Pex19p. J. Biol. Chem. *281*:36-42.

Matsuzono, Y., Matsuzaki, T., and Fujiki, Y. 2006. Functional domain mapping of peroxin Pex19p: interaction with Pex3p is essential for function and translocation. J. Cell Science *119*: 3539-3550.

Mayerhofer, P.U., Kattenfeld, T., Roscher, A.A., Muntau, A.C. 2002. Two splice variants of human PEX19 exhibit distinct functions in peroxisomal assembly. Biochem. Biophys. Res. Commun. *291*:1180-6.

Meinecke, M., Cizmowski, C., Schliebs, W. Krüger, V., Beck, S., Wagner, R., and Erdmann, R. 2010. The peroxisomal importomer constitutes a large and highly dynamic pore. Nat. Cell Biol. *12*:273-7.

Michels, P.A., Moyersoen, J., Krazy, H., Galland, N., Herman, M., and Hannaert, V. 2005. Peroxisomes, glyoxysomes, and glycosomes. Mol. Membr. Biol. *22*:133-45.

Nelson, B.K., Cai, X., and Nebenführ, A. 2007. A multicolored set of *in vivo* organelle markers for co-localization studies in *Arabidopsis* and other plants. Plant J. *51*:1126-1136.

Nito, K., Kamigaki, A., Kondo, M., Hayashi, M., and Nishimura, M. 2007. Functional classification of *Arabidopsis* peroxisome biogenesis factors proposed from analyses of knockdown mutants. Plant Cell Phys. *48*:763-774.

Otzen, M., Perband, U., Wang, D., Baerends, R.J., Kunau, W.H., Veenhuis, M., and Van der Klei, I.J. 2004. *Hansenula polymorpha* Pex19p is essential for the formation of functional peroxisomal membranes. J. Biol. Chem. *279*:19181-90.

Pracharoenwattana, I., Cornah, J.E., and Smith, S.M. 2007. *Arabidopsis* peroxisomal malate dehydrogenase functions in β-oxidation but not in the glyoxylate cycle. Plant J. *50*:381–390.

Ramón, N.M. and Bartel, B. Interdependence of the peroxisome-targeting receptors in *Arabidopsis thaliana*: PEX7 facilitates PEX5 accumulation and import of PTS1 cargo into peroxisomes. Mol. Biol. Cell *21*:1263-1271.

Rottensteiner, H., Kramer, A., Lorenzen, S., Stein, K., Landgraf, C., Volkmer-Engert, R., and Erdmann, R. 2004. Peroxisomal membrane proteins contain common Pex19p-binding sites that are an integral part of their targeting signals. Mol. Biol. Cell *15*:3406-17.

Rucktäschel, R., Thoms, S., Sidorovitch, V., Halbach, A., Pechlivanis, M., Volkmer, R., Alexandrov, K., Kuhlmann, J., Rottensteiner, H., and Erdmann, R. 2009. Farnesylation of Pex19p is required for its structural integrity and function in peroxisome biogenesis. J. Biol. Chem. *284*:20885-20896.

Running, M.P., Fletcher, J.C., and Meyerowitz, E.M. 1998. The WIGGUM gene is required for proper regulation of floral meristem size in *Arabidopsis*. Development *125*:2545-2553.

Running, M.P., Lavy, M., Sternberg, H., Galichet, A., Gruissem, W., Hake, S., Ori, N., and Yalovsky, S. 2004. Enlarged meristems and delayed growth in *plp* mutants result from lack of CaaX prenyltransferases. Proc. Natl. Acad. Sci. *101*:7815-7820.

Sacksteder, K.A., Jones, J.M., South, S.T., Li, X., Liu, Y., and Gould, S.J. 2000. PEX19 binds multiple peroxisomal membrane proteins, is predominantly cytosolic, and is required for peroxisome membrane synthesis. J. Cell Biol. *148*:931-44.

Schliebs, W. and Kunau, W.H. 2004. Peroxisome membrane biogenesis: the stage is set. Curr. Biol. *14*:R397–R409.

Schumann, U., Wanner, G., Veenhuis, M., Schmid, M., and Gietl, C. 2003. AthPEX10, a nuclear gene essential for peroxisome and storage organelle formation during *Arabidopsis* embryogenesis. PNAS *100*:9626-31.

Schuhmann, H., Huesgen, P.F., Gietl, C., and Adamska, I. 2008. The DEG15 serine protease cleaves peroxisomal targeting signal 2-containing proteins in *Arabidopsis*. Plant Phys. *148*:1847-1856.

Sessions, A., Burke, E., Presting, G., Aux, G., McElver, J., Patton, D., Dietrich, B., Ho, P., Bacwaden, J., Ko, C., Clarke, J.D., Cotton, D., Bullis, D., Snell, J., Miguel, T., Hutchison, D., Kimmerly, B., Mitzel, T., Katagiri, F., Glazebook, J., Law, M., and Goff, S.A. 2002. A high-throughput *Arabidopsis* reverse genetic system. Plant Cell *14*:2985-2994.

Sparkes, I. A., Brandizzi, F., Slocombe, S. P., El-Shami, M., Hawes, C., and Baker, A. 2003. An *Arabidopsis pex10* null mutant is embryo lethal, implicating peroxisomes in an essential role during plant embryogenesis. Plant Physiol. *133*:1809-1919.

Stasinopoulos, T. C., and Hangarter, R. P. 1990. Preventing photochemistry in culture media by long-pass light filters alters growth of cultured tissues. Plant Physiol. *93*:1365-9.

Strader, L.C., Culler, A.H., Cohen, J.D., and Bartel, B. 2010. Conversion of endogenous indole-3-butyric acid to indole-3-acetic acid drives cell expansion in *Arabidopsis* seedlings. Plant Phys. *153*:1577-1586.

van der Zand, A., Braakman, I., and Tabak, H.F. 2010. Peroxisomal membrane proteins insert into the endoplasmic reticulum. Mol. Biol. Cell *21*:2057-2065.

Vastiau, I.M.K., Anthonio, E.A., Brams, M., Brees, C., Young, S.G., Van de Velde, S., Wanders, R.J.A., Mannaerts, G.P., Baes, M., Van Veldhoven, P.P., and Fransen, M. 2006. Farnesylation of Pex19p is not essential for peroxisome biogenesis in yeast and mammalian cells. Cell. Mol. Life Sci. *63*:1686-1699.

Vaucheret, H., Béclin, C., Elmayan, T., Feuerbach, F., Godon, C., Morel, J.B., Mourrain, P., Palauqui, J.C., and Vernhettes, S. 1998. Transgene-induced gene silencing in plants. Plant J. *16*:651-9.

Winter, D., Vinegar, B., Nahal, H., Ammar, R., Wilson, G.V., and Provart, N.J. 2007. An "Electronic Fluorescent Pictograph" browser for exploring and analyzing large-scale biological data sets. PLoS One *8*:e718.

Woodward, A.W. and Bartel, B. 2005. Auxin: regulation, action, and interaction. Annals of Botany *95*:707-735.

Yalovsky, S., Kulukian, A., Rodriguez-Concepcion, M., Young, C.A., and Gruissem, W. 2000. Functional requirement of plant farnesyltransferase during development in *Arabidopsis*. Plant Cell *12*:1267-1278.

Zolman, B.K., Yoder, A., and Bartel, B. 2000. Genetic analysis of indole-3-butyric acid responses in *Arabidopsis thaliana* reveals four mutant classes. Genetics *156*:1323-1337.

Zolman, B.K. and Bartel, B. 2004. An *Arabidopsis* indole-3-butyric acid-response mutant defective in PEROXIN6, an apparent ATPase implicated in peroxisomal function. PNAS *101*:1786-1791.

Zolman, B.K., Monroe-Augustus, M., Silva, I.D., Bartel, B. 2005. Identification and characterization of *Arabidopsis* PEROXIN4 and the interacting protein PEROXIN22. Plant Cell *17*:3422-35.